

## Article

# Heat Mitigation Benefits of Street Tree Species during Transition Seasons in Hot and Humid Areas: A Case Study in Guangzhou

Senlin Zheng<sup>1,2</sup>, Caiwei He<sup>2</sup>, Haodong Xu<sup>1</sup>, Jean-Michel Guldmann<sup>3</sup>  and Xiao Liu<sup>4,5,6,\*</sup> 

<sup>1</sup> School of Water Conservancy and Civil Engineering, South China Agricultural University, Wushan Road 483, Guangzhou 510642, China; zhengsl@scau.edu.cn (S.Z.)

<sup>2</sup> School of Civil and Transportation Engineering, Guangdong University of Technology, Outer Ring West Road 100, Guangzhou 510006, China

<sup>3</sup> Department of City and Regional Planning, The Ohio State University, Columbus, OH 43210, USA; guldmann.1@osu.edu

<sup>4</sup> State Key Laboratory of Subtropical Building and Urban Science, South China University of Technology, Guangzhou 510641, China

<sup>5</sup> School of Architecture, South China University of Technology, Guangzhou 510641, China

<sup>6</sup> Faculty of Architecture, The University of Hong Kong, Hong Kong 999077, China

\* Correspondence: xiaoliu@scut.edu.cn

**Abstract:** The potential microclimatic effects of street trees are influenced by their ecological characteristics, planting patterns, and street orientations, especially in subtropical hot and humid areas. To investigate these effects, four typical street tree species in Guangzhou were selected for study during the transition seasons: *Khaya senegalensis*, *Terminalia neotaliala*, *Ficus microcarpa*, and *Mangifera indica*. Air temperature (AT), relative humidity (RH), solar radiation (SR), surface temperature (ST), wind speed (WS), and the leaf area index (LAI) were monitored. The cooling effects of these four species and the resulting improvements in human thermal comfort (HTC) were assessed. The influences of tree planting patterns and street orientations on cooling benefits were systematically analyzed. The results indicate that, during transition seasons, the four street trees, on average, can block 96.68% of SR, reduce AT by 1.45 °C and ST by 10.25 °C, increase RH by 5.26%, and lower the physiologically equivalent temperature (PET) by 8.34 °C. *Terminalia neotaliala*, reducing AT and PET by 1.76 °C and 12.4 °C, respectively, offers the greatest potential for microclimate improvement. Among the four tree species, the variations in ST ( $\Delta$ ST) and PET ( $\Delta$ PET) were minimal, at only 0.76 °C and 0.25 °C, respectively. The average differences in AT and PET between inter-tree and under-tree environments were 0.06 °C and 0.98 °C, respectively. The AT reduction rate was 1.7 times higher in the double-row planting pattern compared to the single-row planting pattern. Street trees planted in the northwest–southeast (NW–SE) orientation exhibited a 16.96% lower WS reduction than those in other orientations. The northeast–southwest (NE–SW) orientation showed the least potential to enhance human thermal comfort. Compared to NE–SW, the northwest–southeast (NW–SE) orientation achieved twice the rate of AT reduction, while the north–south (N–S) orientation improved it by 1.3 times. This data analysis aids in assessing the impact of green infrastructure on urban climates and demonstrates the year-round microclimatic benefits of street trees.

**Keywords:** urban microclimate; transition season; street orientation; street trees; planting patterns



**Citation:** Zheng, S.; He, C.; Xu, H.; Guldmann, J.-M.; Liu, X. Heat Mitigation Benefits of Street Tree Species during Transition Seasons in Hot and Humid Areas: A Case Study in Guangzhou. *Forests* **2024**, *15*, 1459. <https://doi.org/10.3390/f15081459>

Academic Editor: Marcello Vitale

Received: 10 July 2024

Revised: 3 August 2024

Accepted: 13 August 2024

Published: 19 August 2024



**Copyright:** © 2024 by the authors. Licensee MDPI, Basel, Switzerland. This article is an open access article distributed under the terms and conditions of the Creative Commons Attribution (CC BY) license (<https://creativecommons.org/licenses/by/4.0/>).

## 1. Introduction

Rapid urban expansion, population pressure, fossil fuel consumption, and inadequate urban vegetation have resulted in urban areas being typically warmer than rural areas, a phenomenon known as the urban heat island (UHI) effect [1,2]. The cooling effect of vegetation on urban surfaces is diminished by the reduction in wetlands and the replacement of traditional natural surfaces with impermeable substrates [3]. Changes in the urban

thermal environment have altered the energy balance of cities, leading to increased energy consumption and serious health problems for urban dwellers [4–7].

Sidewalks are an important setting for human activities [8], and planting sidewalk trees has become an important means to alleviate the UHI effect. Compared with lawns, trees have a stronger effect in improving the thermal environment of urban street canyons [9]. First, trees effectively mitigate outdoor thermal stress by absorbing and blocking solar radiation [10,11], creating shadows and reducing long-wave radiation exchanges between the ground and the surrounding buildings [12,13]. Through leaf transpiration, trees can also reduce the leaf surface temperature and air temperature, as well as increase air humidity [14,15]. However, when encountering extremely high-temperature weather, leaf stomata close partially out of a protective mechanism, reducing water vapor emission and weakening the transpiration cooling effect [16]. Shading and transpiration are the main means of vapor heat stress mitigation in trees, but street tree shading plays a more important role. Trees rely primarily on the canopy to reduce downward solar radiation [17], especially visible and infrared light [18,19]. Coutts found that the cooling and human thermal comfort (HTC) benefits of street trees are largely dependent on the degree of shading provided by trees and are localized [20]. Some studies have confirmed that the structural characteristics of trees, such as canopy width, canopy shape, canopy permeability, leaf size and shape, and branch structure [21–23], all affect the performance of the canopy in improving the thermal environment. Then, the leaf area index (LAI) describes the canopy density and is widely used to assess the canopy filtering effect. However, the LAI varies among different tree species and even among trees of the same species [24–26]. As a result, shading performance varies among tree species, with variations in microclimatic benefits [27].

Second, the potential of street trees to regulate the microclimate is closely related to local climatic conditions and street geometry. Eight typical cities in temperate monsoon and Mediterranean climates were investigated by Yu et al. [28], who reported that the cooling effect of green vegetation was weaker in areas with higher relative humidity (RH), whereas increased wind speed can improve thermal efficiency in tropical and subtropical climates [29,30]. Several studies show that street orientation also plays a key role in the UHI effect, directly affecting the solar distribution and airflow in urban street canyons. Different urban structures, street aspect ratios (H/W ratios), and directions have different impacts on UHI mitigation [31,32]. For example, there are differences in the cooling effect of vegetation between north–south streets and east–west streets [33], but the effects of different street directions and aspect ratios on the thermal performance of buildings were also found to be inconsistent [34]. Understanding to what degree native tree species in different areas are able to provide microclimatic benefits for urban dwellers and pedestrians under different street orientations is extremely important for urban street tree selection and replacement.

Third, trees planted in clusters are more effective in improving the microclimate than isolated, individual trees [35–37]. Abreu-Harbich et al. [22] showed that a single tree can reduce the air temperature (AT) by 0–2.8 °C during a given summer period in Brazil, while clustered trees can reduce AT by 0.3–15.7 °C. Park et al. observed that the effect of median strip tree vegetation on wind speed and air temperature is slight when compared to street trees planted on the sidewalk [38]. It is evident that the microclimatic benefits of trees vary across different planting configurations [39,40].

Many researchers have conducted extensive research on trees as a means to mitigate the UHI effect and improve HTC [41–45]. The cooling effects of trees have been quantified by experimental measurements and numerical simulations. In order to more accurately simulate planting scenarios, numerical simulation studies need to be supported by a large number of field measurements of different native tree species [43,44,46]. Currently, the most relevant studies are focused on tropical and temperate climates, with fewer studies on subtropical climates. Generally, when measuring microclimatic parameters, the typical hottest (coldest) months are chosen, with less attention to other seasons, such as transitional seasons with cloudy and rainy weather. It is noteworthy that the subtropical monsoon climate is characterized by high temperatures and heavy rainfall in transition seasons, but

the microclimatic behavior of trees during this period has been overlooked. In addition, most studies have monitored microclimatic parameters under street trees, without exploring the inter-tree microclimatic behavior.

In this study, focusing on the subtropical transition season, five microclimatic factors (air temperature and humidity, solar radiation, wind speed, and surface temperature) are analyzed, in conjunction with street orientations and planting patterns, to evaluate the microclimatic benefits and explore the inter-tree microclimatic behavior, using of four typical street trees in hot and humid areas.

The research objectives include (1) quantifying the cooling effects and microclimatic advantages of these species; (2) examining the disparities in microclimatic advantages between inter-tree and under-tree environments; (3) assessing the influence of planting patterns on the microclimatic responses of street trees; and (4) exploring the variations in cooling effects across different street orientations.

The research findings will (1) be critical for developing urban design guidelines for climate adaptation in subtropical urban areas; (2) address knowledge gaps regarding the microclimate benefits of street trees during transition seasons; and (3) contribute to reducing the costs of urban forestry management.

## 2. Methodology

Following the literature review, field surveys, and in situ measurements, we have analyzed the effects of different street tree species, planting patterns, and street orientations on the microclimate beneath trees during transition seasons, based on field test data. The methodological flowchart is presented in Figure 1.

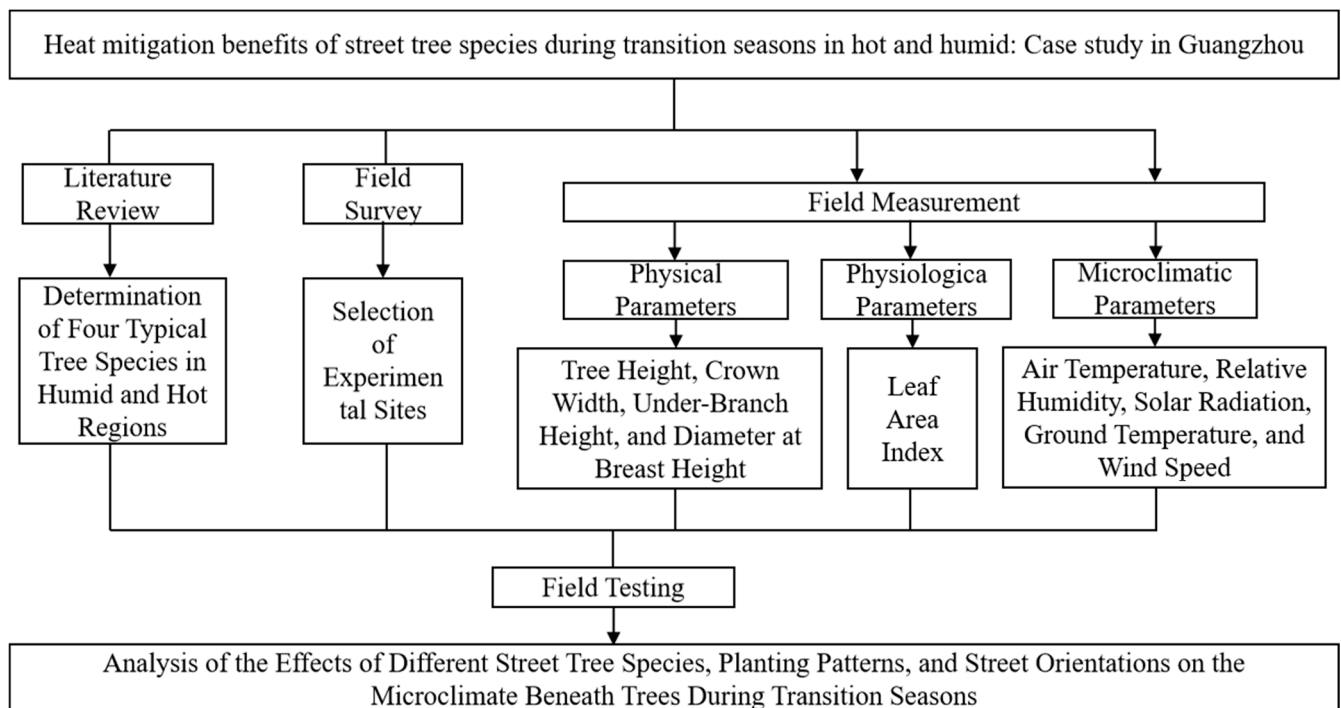


**Figure 1.** Methodological flowchart.

### 2.1. Study Area and Climate

This study was conducted at the Guangzhou Higher Education Mega Center, characterized by a hot and humid climate. Guangzhou (23.13° N, 113.27° E) is situated in a subtropical monsoon climate, classified as the Cfa climate type according to the Köppen classification. Summers are characterized by high temperatures, high humidity, and strong rainfall, often accompanied by short-lived gales and heavy precipitation, while winters are mild, cool, and dry. Air temperature (AT), relative humidity (RH), and precipitation data

for a typical year are illustrated in Figure 2a. The hottest month is July, with an average air temperature of 30.3 °C, relative humidity of 74.1%, and rainfall of 67.5 mm; the coldest month is December, with an average air temperature of 14.6 °C, relative humidity of 68.8%, and rainfall of 1.9 mm. The annual maximum air temperature can reach 37.9 °C, with the highest monthly average solar radiation in July (475.22 MJ/m<sup>2</sup>) and the lowest in February (226.67 MJ/m<sup>2</sup>) [47]. The annual average relative humidity exceeds 68%. Influenced by the monsoon climate, the prevailing wind directions are highly seasonal, with southeast winds in summer and northern winds in winter (Figure 2b). Situated in the Pearl River Delta region, a zone frequently affected by tropical cyclones, Guangzhou experiences persistent heavy rainfall during the transition season from May to June, with daily maximum air temperatures exceeding 35 °C and average precipitations of 283.6 mm and 257.7 mm in May and June, respectively [48]. These climatic features distinctly characterize the subtropical monsoon climate. Consequently, to investigate the microclimatic effects of street tree species under typical cloudy conditions during transitional seasons, tests were conducted from June 3 to 10, with cloud cover ranging from 40% to 70%.

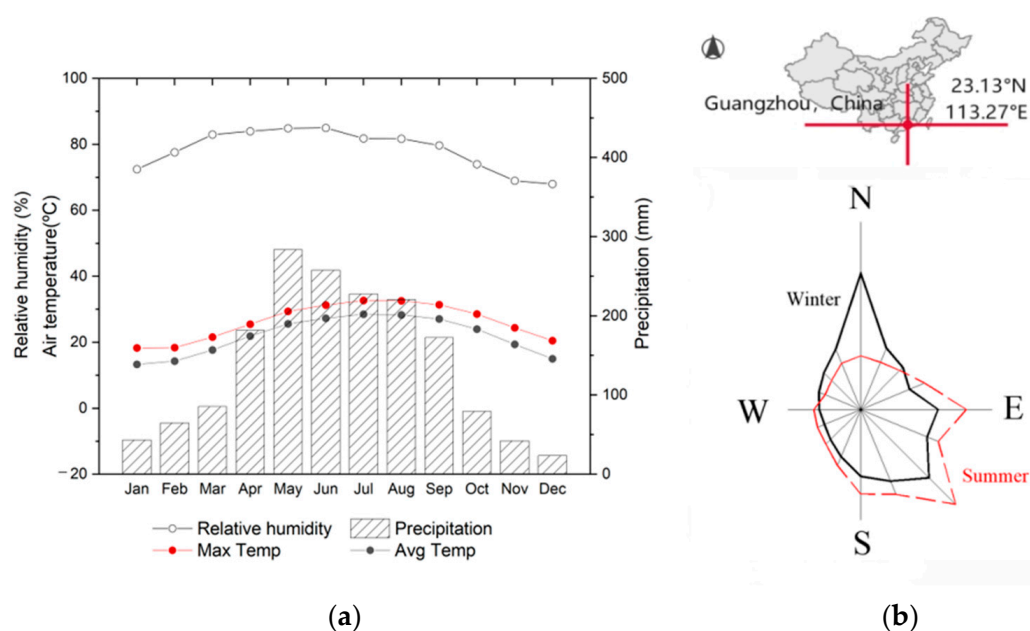


**Figure 2.** (a) Meteorological data for a typical year; (b) wind rose diagram in Guangzhou (China Meteorological Data Service Center, 2020).

## 2.2. Study Subjects

The urban forest of Guangzhou Higher Education Mega Center covers a wide area, where street trees account for 27.76% of all tree species, and includes up to 29 street tree species, with the most common ones described in Table 1 [49]. In order to retain distinct morphological attributes, four typical street trees were selected: *Khaya senegalensis*, *Terminalia neotaliala*, *Ficus microcarpa*, and *Mangifera indica* (Figure 3). The main morphological attributes of these trees are presented in Table 2. Based on field conditions, trees planted in rows and growing well were selected as test objects. In order to ensure that only the tree has an impact on the microclimate, the test was conducted in an open field without buildings or other shelters in proximity. Pavements were adopted for the underlying surface of the study site.

Street orientations parallel (northwest–southeast, NW–SE), perpendicular (northeast–southwest, NE–SW), and offset (north–south, N–S) to the prevailing wind direction in Guangzhou were selected for this study. The specifics of each of the four study sites are presented in Figure 4: (1) single-row *Khaya senegalensis*: NE–SW; (2) single-row *Terminalia neotaliala*: NW–SE; (3) double-row *Ficus microcarpa* and *Mangifera indica*: N–S; and (4) double-row *Ficus microcarpa*: NE–SW. The canopy cover above the road (CCAD) and the LAI are

the two factors that mainly affect the thermal comfort under the canopy [50]. To study the effects of street orientations, it was ensured that the CCAD and the LAI under the canopy were comparable across the test sites (1), (2), (3), and (4).

**Table 1.** Most common street tree species in the study area [49].

Number	Species	Family and Genus	Number of Trees	Proportion (%)
1	<i>Ficus microcarpa</i>	Moraceae Ficus	775	25.7
2	<i>Syzygium hainanense</i>	Myrtaceae Syzygium	283	9.4
3	<i>Khaya senegalensis</i>	Meliaceae Melia	253	8.4
4	<i>Bauhinia</i>	Leguminosae Bauhinia	141	4.7
5	<i>Terminalia neotaliala</i>	Combretaceae Terminalia	136	4.5
6	<i>Mangifera indica</i>	Sumac Mangifera	59	2.0

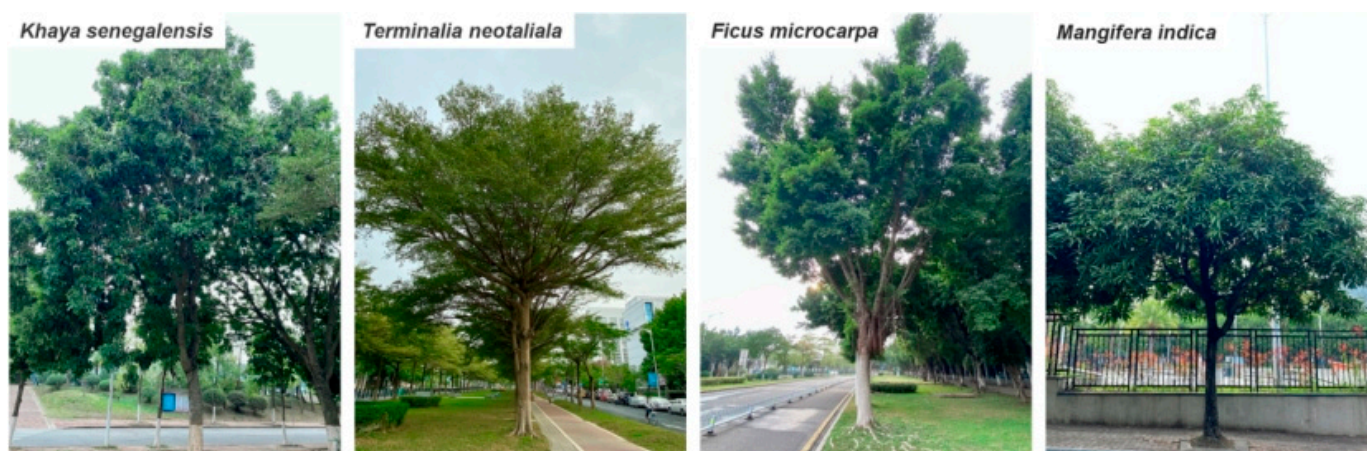


**Figure 3.** Tested street tree species.

**Table 2.** Physical parameters of the tested tree species.

Species	Height (m)	Height below Branch (m)	Trunk Diameter (m)	Canopy Diameter (m)	Leaf Area Index (m <sup>2</sup> /m <sup>2</sup> )
<i>Khaya senegalensis</i>	12.39	2.80	0.31	9.90	4.11
<i>Terminalia neotaliala</i>	10.40	4.17	0.26	10.90	4.37
<i>Mangifera indica</i>	9.67	2.47	0.23	6.82	1.94
<i>Ficus microcarpa</i>	11.49	2.54	0.39	9.42	5.69

### 2.3. Field Measurements

Air temperature and humidity, solar radiation, surface temperature, and wind speed are the primary factors influencing outdoor human thermal comfort (HTC) [51,52]. In addition to microclimatic parameters, physical characteristics such as tree height, canopy diameter and shape also play a crucial role in enhancing human thermal comfort (HTC) [53,54]. Consequently, in this study, we measured the air temperature and humidity, solar radiation, surface temperature, wind speed, tree height, canopy diameter, trunk diameter, and leaf area index (LAI) of street trees. The measuring instruments and their principal technical parameters are detailed in Table 3.

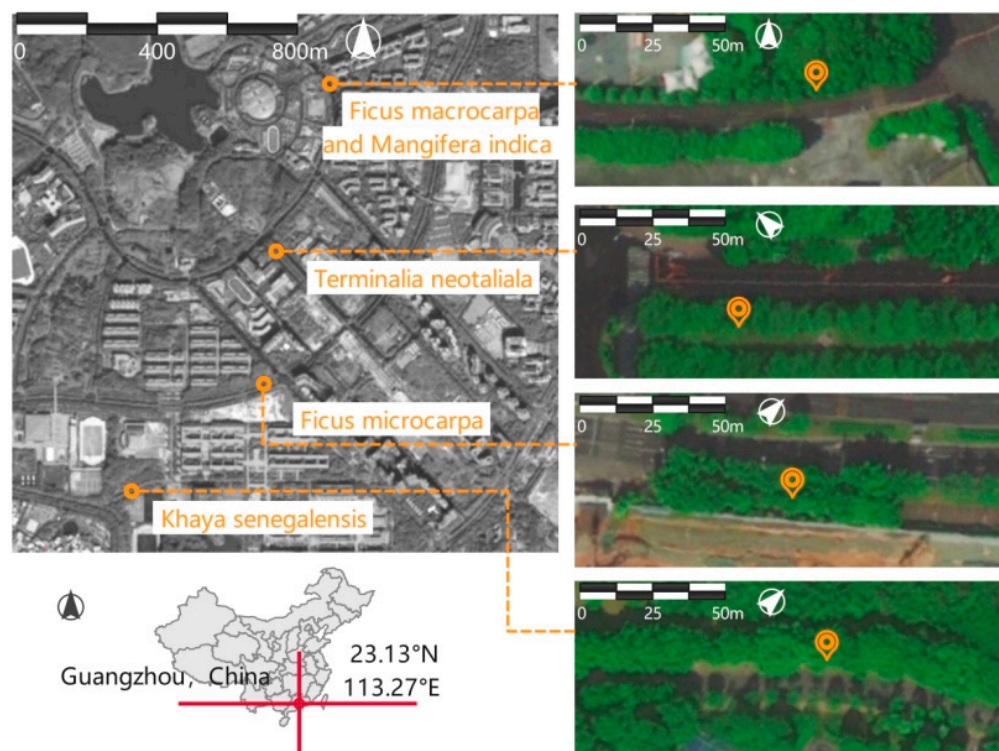


**Figure 4.** Location and orientation of the experimental test sites.

**Table 3.** Variables and instruments used in field measurements.

Elements	Instruments	Manufacturer	Accuracy	Measurement Range	Sampling
Air temperature and humidity	HOBO data logger (U23-001)	Onset Computer Corporation, Bourne, MA, USA	$\pm 0.2\text{ }^{\circ}\text{C}$ (0~50 h)	$-40\text{ }^{\circ}\text{C}\sim 70\text{ }^{\circ}\text{C}$	5 min
Surface temperature	HOBO Thermocouple				
Solar radiation under trees	Two-component radiation sensor	Hukseflux Company, Delft, The Netherlands	$\leq 5\%$	$0\sim 2000\text{ W/m}^2$	5 min
Solar radiation between trees			--		
Wind speed	HD32.3 thermal environment analyzer	M. Young Company, Traverse, MI, USA	Class 1/3 DIN $\pm 0.05\text{ m/s}$	$-10\text{ }^{\circ}\text{C}\sim 100\text{ }^{\circ}\text{C}$ $0\sim 5\text{ m/s}$	5 min
Black globe temperature					
Weather parameters	Davis Vantage Pro2	Davis Company, Boston, MA, USA	$\pm 0.6\text{ }^{\circ}\text{C}$ (Ta) $\pm 3\%$ (RH) $\pm 5\%$ (S,V)	$-40\sim 65\text{ }^{\circ}\text{C}$ (Ta) $0\sim 1800\text{ W/m}^2$ (S)	10 min

Measuring points were situated in the center of the pavement. Under-tree and inter-tree measuring points, positioned 1.5 m above the ground, were used to assess fluctuations in microclimatic parameters (Figure 5). Parameter values in shaded areas beneath trees were averaged from both under-tree and inter-tree measuring points. Additionally, measuring points were established in open areas devoid of buildings to serve as references. In the experiment, three points under the trees and two between them were designated during field measurements; to ensure parameter accuracy, three instruments were positioned at each point for comparative analysis. Temperature, humidity, solar radiation, wind, and other experimental data were analyzed by averaging the values and eliminating anomalies, thereby accurately reflecting the actual microclimatic environment of the experimental site.

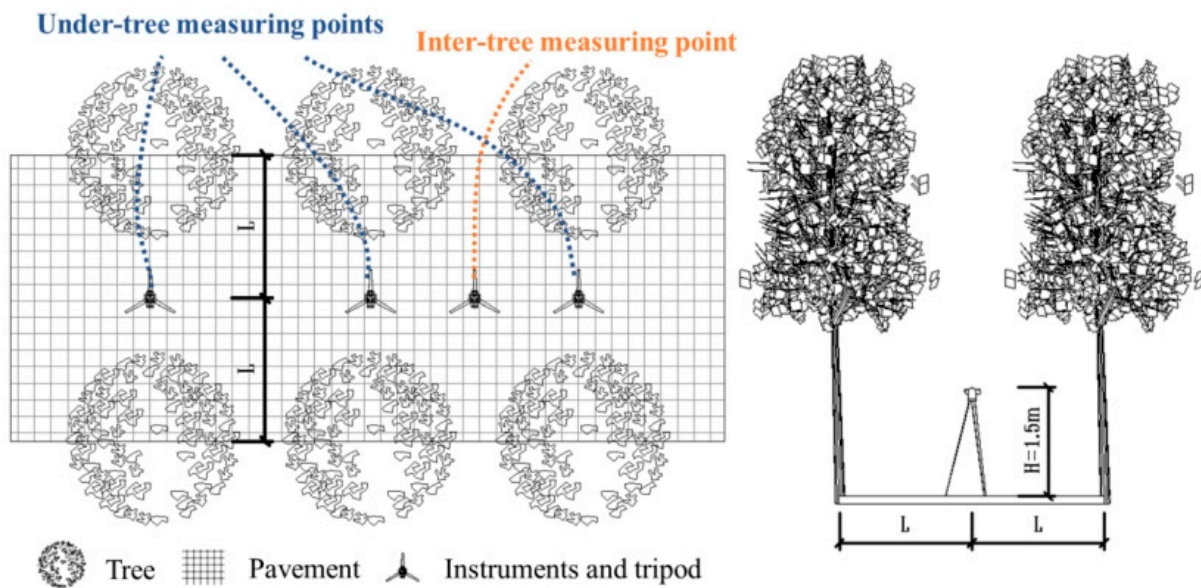


**Figure 5.** Schematic diagram of measuring points.

In this experiment, microclimatic parameters were assessed using a fixed-point measurement method. Air temperature and humidity under the shade were recorded with a HOBO data logger, black bulb temperature and wind speed (WS) were recorded with an HD32.3 thermal environment analyzer, and surface temperature (ST) was recorded with a HOBO thermocouple. Solar radiation was recorded using a short-wave radiation sensor and a two-component radiation sensor, positioned under the tree and between the trees, respectively, with direct solar radiation being the primary consideration. Simultaneously, short-wave and two-component radiation sensors were utilized to record solar radiation (SR) under and between trees. The Davis Vantage Pro2 instrument was employed to record weather parameters in the open area. Microclimatic parameters in the shaded area were logged every 5 min, while meteorological parameters in the open area were logged every 10 min. To prevent radiation interference with air temperature, the HOBO data logger was enclosed in a louvered box radiation shield during measurements (Figure 6a). When measuring surface temperature, thermocouples were evenly coated with thermally conductive silicone grease to ensure optimal contact with the pavement, thereby maintaining data accuracy (Figure 6b).

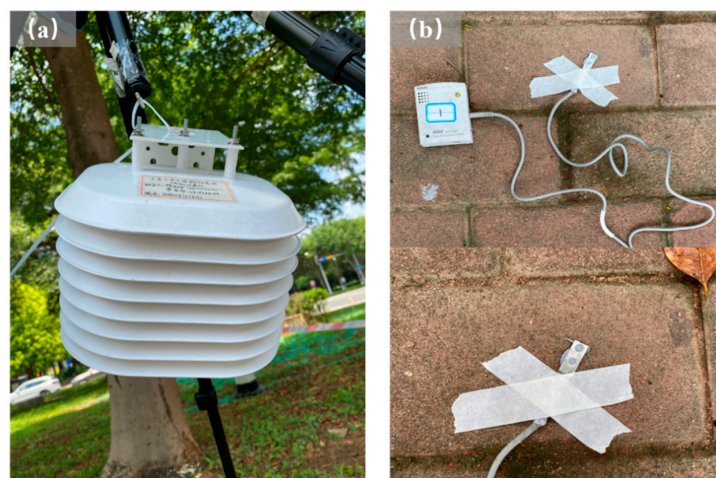


**Figure 6.** Instrument arrangement for experimental testing: (a) Louvered box radiation shield; (b) HOBO thermocouple.

The physical parameters of the trees were measured using a metric ruler. Because tree height is difficult to measure, we used AutoCAD 2022 software to help measure it by placing reference objects beside the trees and taking photographs. However, the LAI was measured with an LAI-2200 Plant Canopy Analyzer (Lincoln, NE, USA) and recalculated by using the FV2200 software V2.1 [55]. The LAI-2200 instrument was moved along parallel bands 1.5 m above the ground under the canopy of the test trees, taking measurements every 2 m. Three measurements were then averaged for each test tree.

### 3. Results and Analysis

#### 3.1. Air Temperature (AT)

Figure 7 shows the daily patterns of AT between the trees, under the trees, and in the open area for the four tree species. (1) The daily patterns of AT between open and shaded areas are consistent, reaching a maximum around 16:00 p.m., but at any time, AT in the open area is significantly higher than in the shaded area. (2) AT in the shaded area generally varies less and is more stable, while AT in the open area varies dramatically. (3) The under-tree and inter-tree AT curves almost overlap for all four tree species, with a mean  $\Delta AT$  of 0.06 °C. From 14:00 to 15:00 p.m.,  $\Delta AT$  for *Ficus microcarpa* between open and shaded areas is very small (Figure 7d), due to the thickening of cloud cover and weaker solar radiation, and subsequently lower AT.

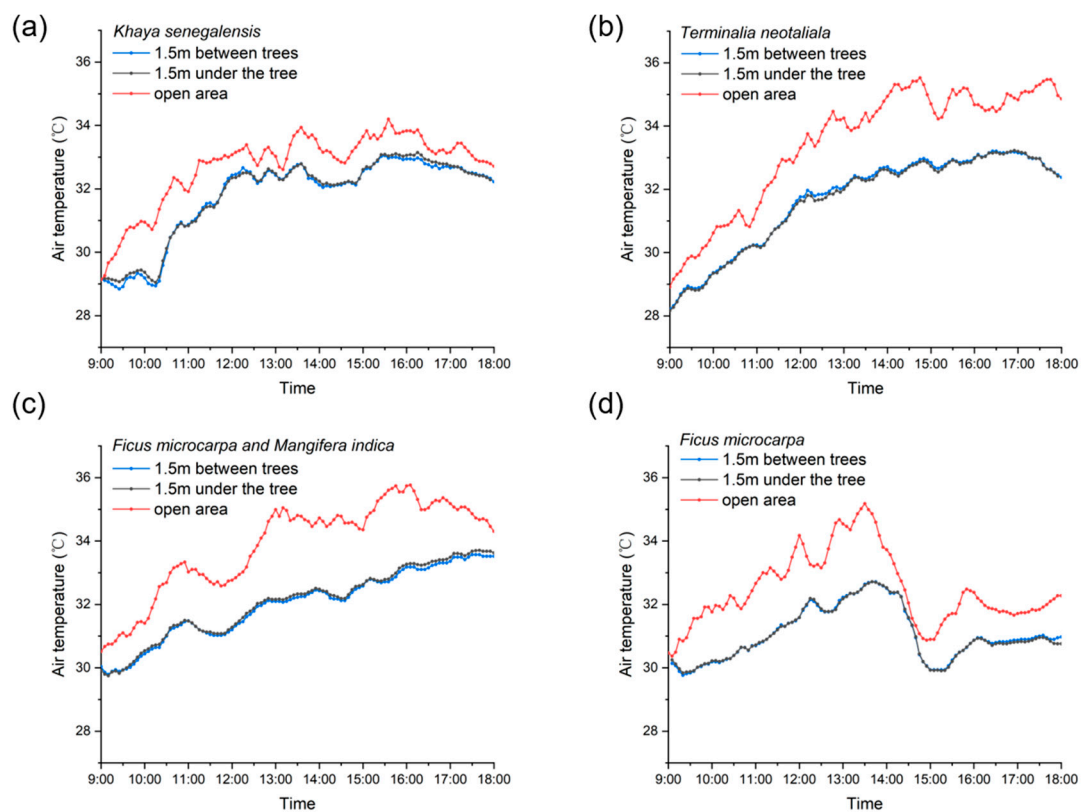


**Figure 7.** Daily variations in AT between trees, under trees, and in the open area at a reference height (1.5 m) for four tree species. (a) is *Khaya senegalensis*, (b) is *Terminalia neotaliala*, (c) is *Mangifera indica*, and (d) is *Ficus microcarpa*.

The extent to which the four tree species contribute to AT is quantified in Figure 8a,b. All trees display a significant effect on cooling the air, with the highest  $\Delta AT$  for *Ficus microcarpa* and *Mangifera indica* (average of 1.82 °C) and *Terminalia neotaliala* (average of 1.76 °C), and the smallest  $\Delta AT$  for *Khaya senegalensis* (average of 0.99 °C).



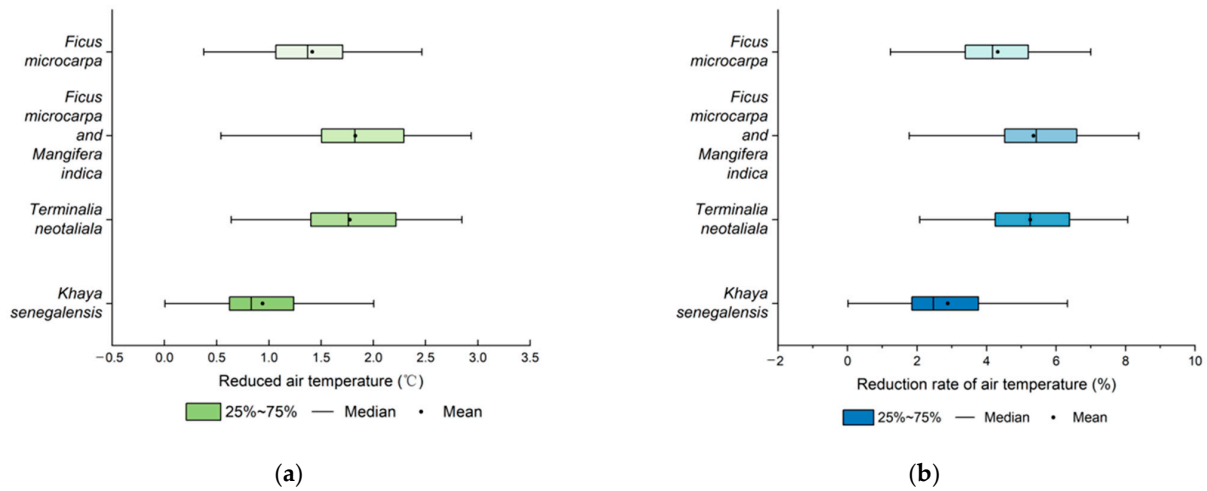


**Figure 8.** Comparison of the air-cooling effect in the shaded area at the reference height (1.5 m) among the four tree species: (a)  $\Delta AT = AT$  in the open area –  $AT$  in the shaded area; (b) reduction rate of  $AT = \Delta AT / AT$  in the open area  $\times 100\%$ .

### 3.2. Relative Humidity (RH)

RH between trees and under trees, and in the open area at a reference height (1.5 m) was measured for the four tree species (Figure 9). (1) Similar to the patterns of AT, the patterns of RH in the open and shaded areas are the same, with consistently higher RH in the shaded area. (2) There are no significant differences in under- and inter-tree RH between the four tree species, with a mean  $\Delta RH$  of 0.44%. (3) RH fluctuates more sharply in the shaded area than in the open area.

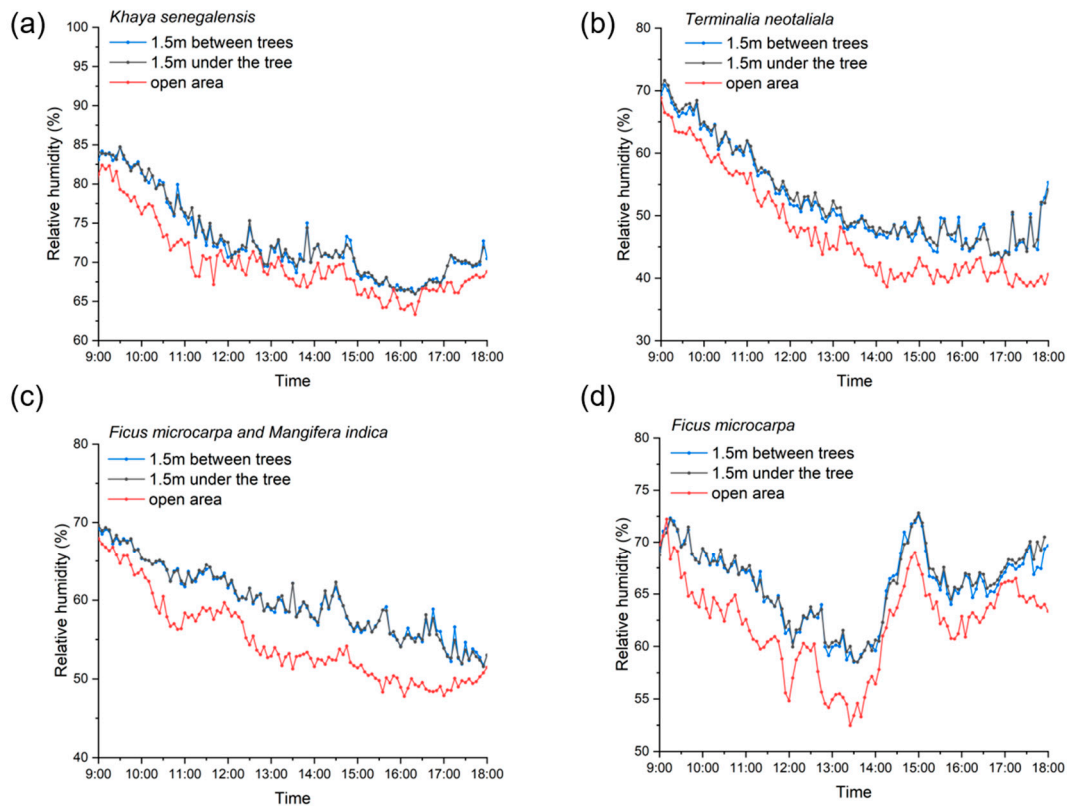


**Figure 9.** Daily variations in RH between trees, under trees, and in the open area at a reference height (1.5 m) among the four tree species. (a) is *Khaya senegalensis*, (b) is *Terminalia neotaliala*, (c) is *Mangifera indica*, and (d) is *Ficus microcarpa*.

The humidifying capacity of the four tree species is illustrated in Figure 10. The average increase in RH ranges from 2.41% to 5.26%. Based on the rate of increase in RH, the largest humidification benefits are obtained with *Terminalia neotaliala* (9.97%), *Ficus microcarpa*, and *Mangifera indica* (9.60%). In contrast, *Ficus microcarpa* (5.98%) and *Khaya senegalensis* (3.51%) are much less effective in enhancing the RH of the air around them. High humidity is evident in the subtropical transition season, and the humidifying capacity of street trees is also influenced by the RH of the actual climatic conditions. Humidification due to vegetation varies with the overall RH; a lower RH rate leads to higher humidification. For the four tree species, RH increases by 5.03% when RH in the open area is below 60%. In contrast, RH increases by only 3.1% when RH in the open area is above 60%. The optimum RH for human survival is between 40% and 60%. The RH under *Ficus microcarpa* and *Khaya senegalensis* trees is above 60%, which may affect pedestrians' HTC.

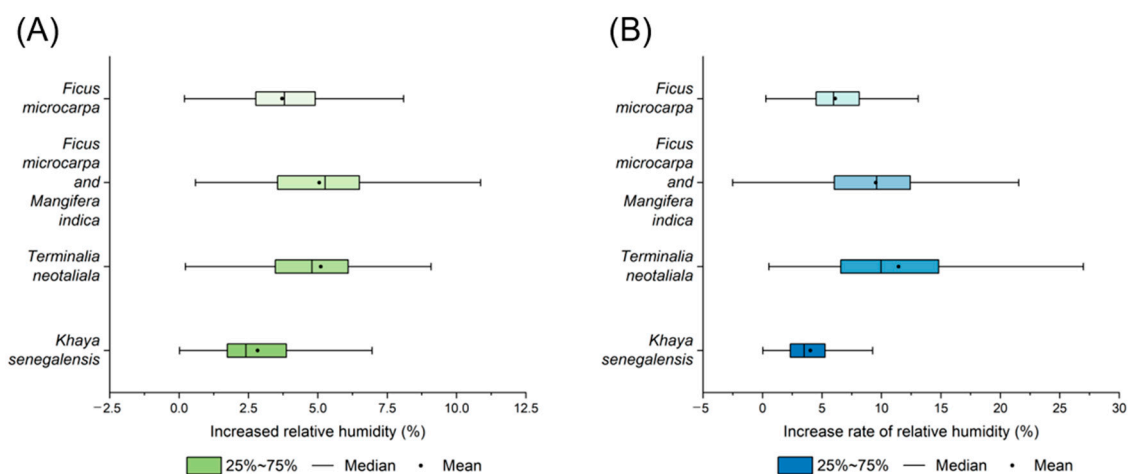


**Figure 10.** Comparison of the rate of increase in RH in the shaded area at reference height (1.5 m) among four tree species: (A)  $\Delta RH = RH$  in the shaded area – RH in the open area; (B) increase rate of RH =  $\Delta RH / RH$  in the open area  $\times 100\%$ .

### 3.3. Solar Radiation (SR)

The daily variations in solar radiation (SR) for the four tree species are documented in Figure 11. When cloudiness is high, SR in the open area exhibits significant instability, with pronounced fluctuations (Figure 11a,c,d), whereas SR fluctuates considerably less under near-clear or less cloudy conditions (Figure 11b). Significant differences in solar radiation (SR) are observed between and beneath trees. SR between trees is stronger and fluctuates more markedly than beneath trees, which is attributed to the phenomenon of light spots. The figure indicates that the under-tree sites receive almost no solar radiation, primarily due to the large crowns of the test trees and the extended duration in which these sites remain shaded.

Trees clearly moderate SR, and the order of SR weakening effectiveness is clear in Figure 12: *Ficus microcarpa* (217.67 W/m<sup>2</sup>, 97.98%), *Mangifera indica* (337.27 W/m<sup>2</sup>, 97.74%), *Khaya senegalensis* (231.06 W/m<sup>2</sup>, 95.87%), and *Terminalia neotaliala* (523.75 W/m<sup>2</sup>, 95.14%). In particular, great differences were found in the stability of diurnal attenuation of SR (Figure 12B). *Ficus microcarpa* and *Mangifera indica* had the strongest stability, while *Terminalia neotaliala*, and *Khaya senegalensis* had the worst stability. This suggests that the tree LAI is a key factor in SR attenuation and maintaining SR stability under the trees.

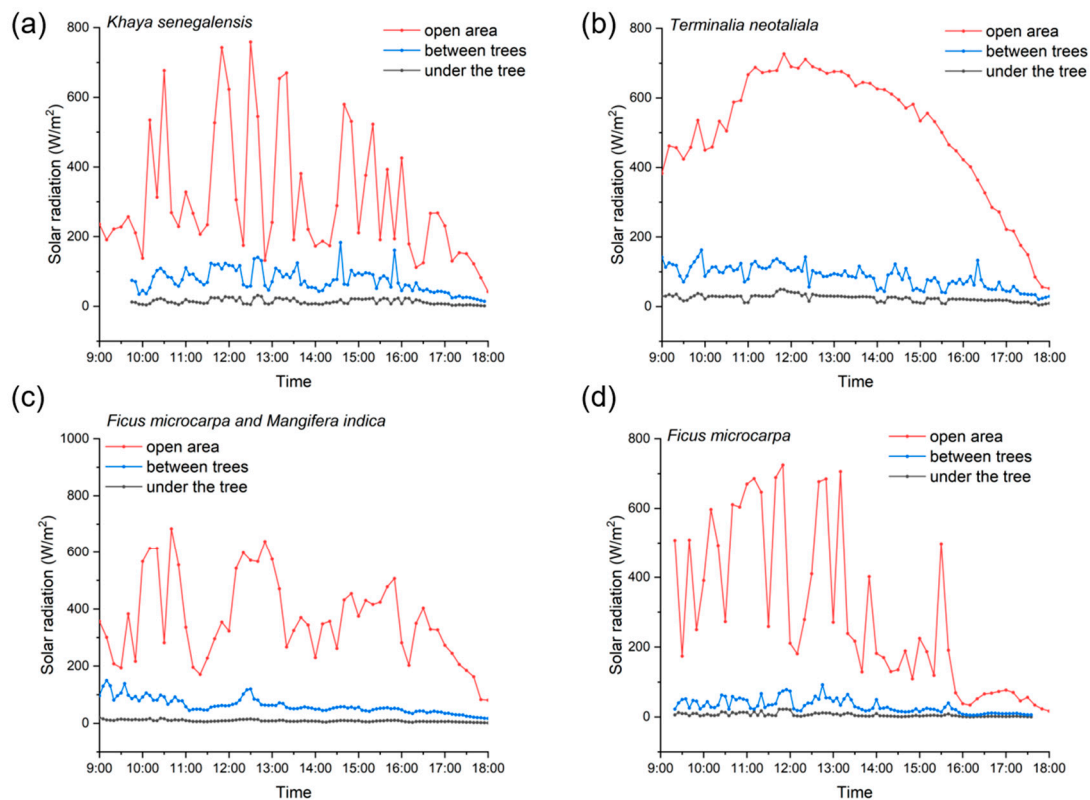


**Figure 11.** Daily variations in SR between trees, under trees, and in the open area for the four tree species. (a) is *Khaya senegalensis*, (b) is *Terminalia neotaliala*, (c) is *Mangifera indica*, and (d) is *Ficus microcarpa*.

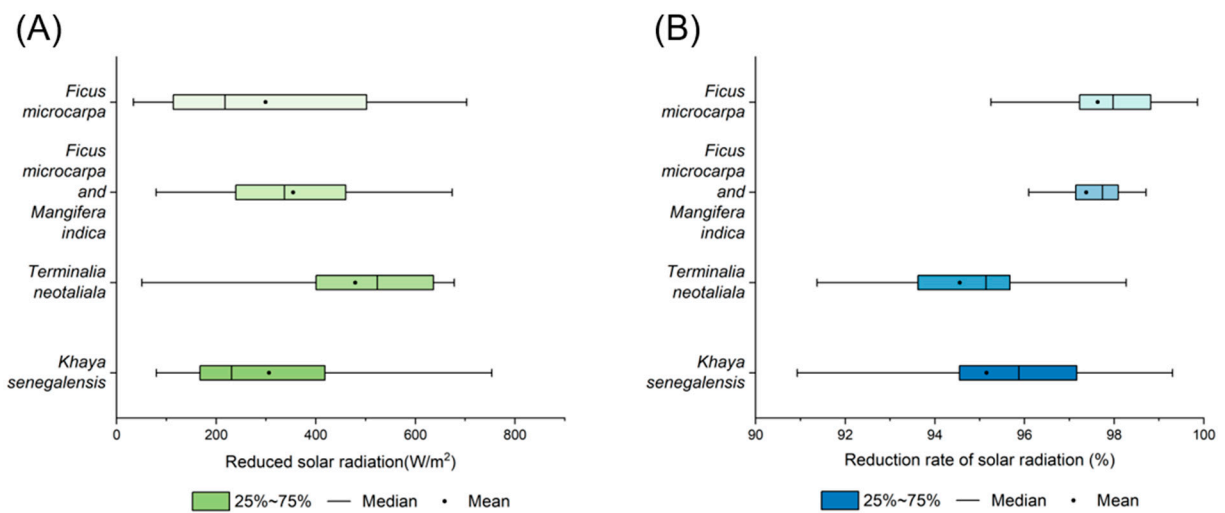


**Figure 12.** Comparison of the degree of SR modification in the shaded area among the four tree species. (A)  $\Delta SR = SR$  in the open area – SR in the shaded area; (B) reduction rate of SR =  $\Delta SR/SR$  in the open area  $\times 100\%$ .

Unlike AT and RH, the under-tree and inter-tree  $\Delta SR$  are significant for the four tree species (Figure 13). The  $\Delta SR$  ranges from 22.01  $W/m^2$  to 65.37  $W/m^2$  (mean 48.26  $W/m^2$ ).

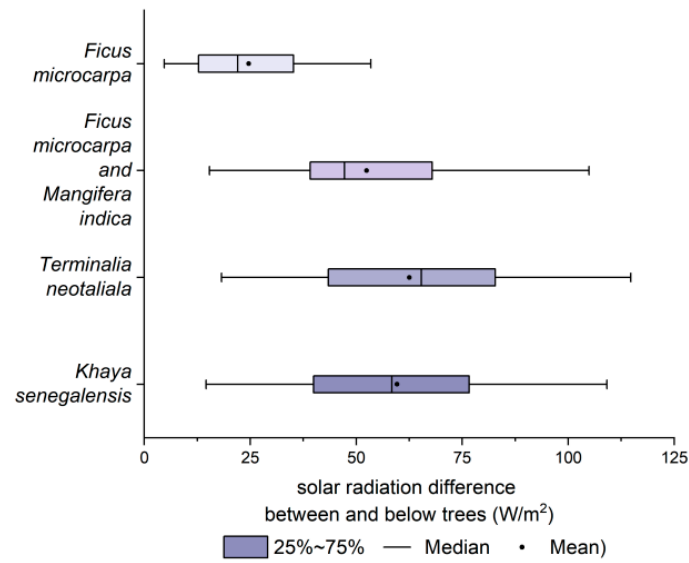


**Figure 13.** Differences between under-tree and inter-tree SR for the four tree species.  $\Delta$ SR = inter-tree SR – under-tree SR.

### 3.4. Surface Temperature (ST)

The underlying surface of the study area is pavement. Due to the shading effect of the tree canopy, the effect of trees on ST is considerable (Figure 14). (1) The pattern of ST is consistent with that of AT. Because of the thermal inertia of ground materials, the ground generally warms up about 10 min later than the air. (2) In the open area, ST is obviously affected by the weather, presenting multiple and drastic fluctuations, while ST in the shaded area has relatively little fluctuation.

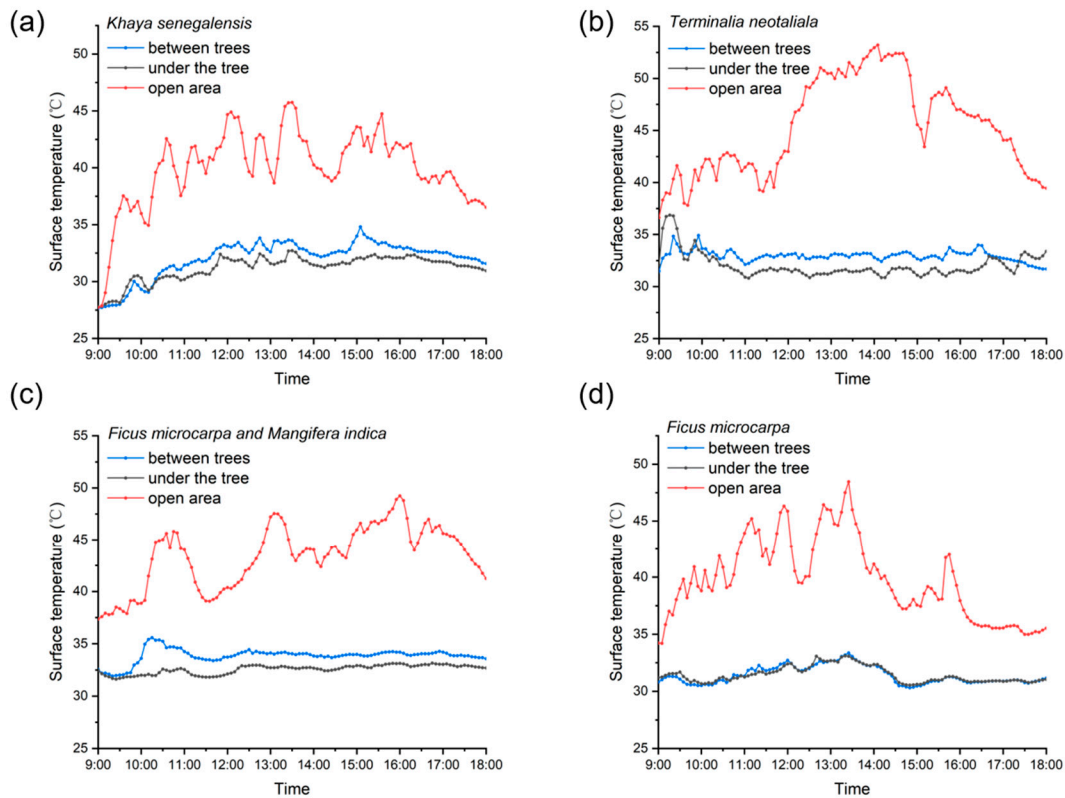


**Figure 14.** Daily variations in ST between trees, under trees, and in the open area for the four tree species. (a) is *Khaya senegalensis*, (b) is *Terminalia neotaliala*, (c) is *Mangifera indica*, and (d) is *Ficus microcarpa*.

The comparison of ST in the open and shaded areas (Figure 15) shows that the cooling benefits reflected by ST vary considerably among the tree species. The greatest cooling benefits are due to *Terminalia neotaliala* (12.9 °C, 28.55%). *Mangifera indica* (11.14 °C, 25.57%) and *Khaya senegalensis* (8.85 °C, 22.46%) generate the next highest cooling benefits. *Ficus microcarpa* (8.09 °C, 20.51%) provides the least cooling benefit.

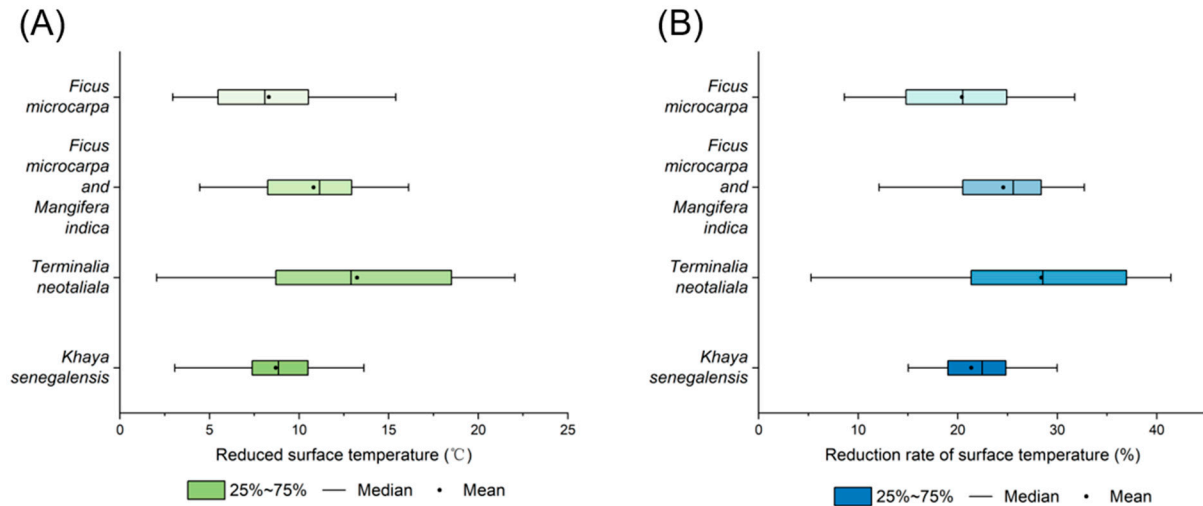


**Figure 15.** Comparison of the degree of reduction in ST in the shaded area among the four tree species. (A)  $\Delta ST = ST$  in the open area –  $ST$  in the shaded area; (B) Reduction rate of  $ST = \Delta ST/ST$  in the open area  $\times 100\%$ .

The analysis of tree species with the same planting pattern and orientation shows that  $\Delta ST$  is 0.76 °C. The range of under-tree and inter-tree  $\Delta ST$  for the four tree species is 0.1 °C–1.42 °C (mean 0.91 °C), with difference rates ranging from 0.33% to 4.46% (mean 2.84%) (Figure 16). The largest under-tree and inter-tree  $\Delta ST$  is observed in *Terminalia neotaliala* and the smallest in *Ficus microcarpa*.

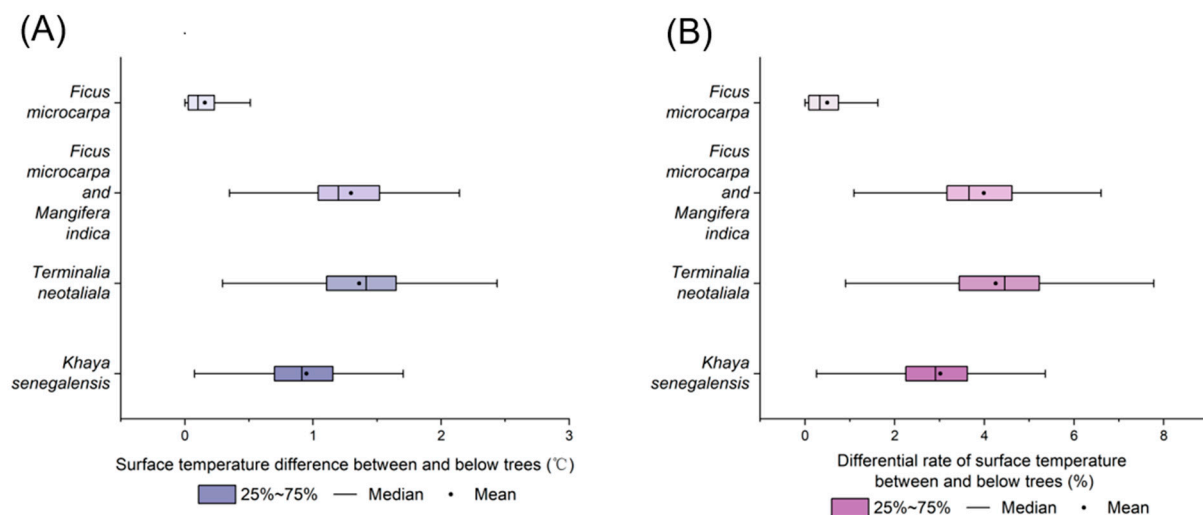


**Figure 16.** Differences between under-tree and inter-tree ST among the four tree species: (A)  $\Delta ST = \text{inter-tree } ST - \text{under-tree } ST$ ; (B) differential rate of  $ST = \Delta ST/\text{under-tree } ST \times 100\%$ .

### 3.5. Wind Speed (WS)

Consistent with previous studies, trees have an obstructive effect on wind. Overall, trees can reduce WS (Figure 17), but this does not mean that WS in the open area is larger than WS in the shaded area at any given time. In fact, WS is occasionally greater in the shaded area (e.g., *Terminalia neotaliala*). Quantifying the WS impeding ability of the four tree

species (Figure 18) reveals that, although there is no significant difference in  $\Delta WS$  among the four tree species (Figure 18A), a noticeable difference in the WS reduction rate is found (Figure 18B). The ranking of the trees in terms of their blocking effect on WS is as follows: *Khaya senegalensis* (0.66 m/s, 51.39%), *Mangifera indica* (0.49 m/s, 44.39%), *Ficus microcarpa* (0.56 m/s, 48.63%), and *Terminalia neotaliala* (0.38 m/s, 31.18%). The average  $\Delta WS$  for the four tree species is 0.52 m/s, and the reduction rate of WS is 43.9%.

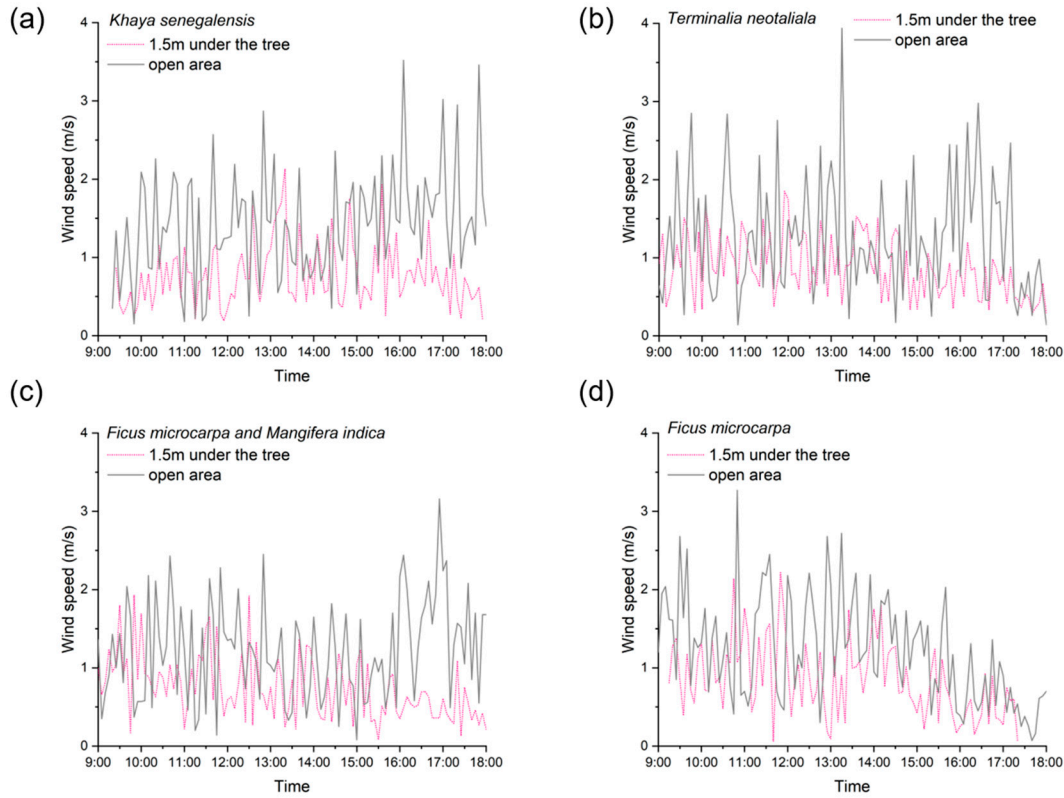


**Figure 17.** Daily variation in WS in open and shaded areas at a reference height (1.5 m) for the four tree species. (a) is *Khaya senegalensis*, (b) is *Terminalia neotaliala*, (c) is *Mangifera indica*, and (d) is *Ficus microcarpa*.

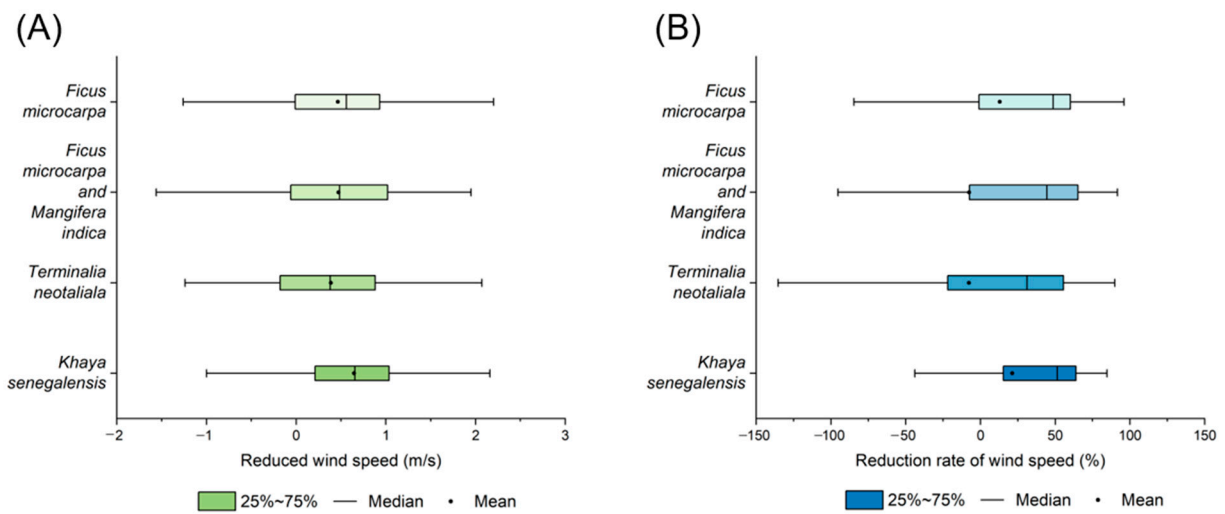


**Figure 18.** Comparison of the degree of reduction in WS in the shaded area among the four tree species: (A)  $\Delta WS = WS$  in the open area – WS in the shaded area; (B) reduction rate of WS =  $\Delta WS / WS$  in the shaded area  $\times 100\%$ .

### 3.6. Physiologically Equivalent Temperature (PET)

The RayMan model, was adopted to evaluate HTC and calculate PET. The current thermal environment considered acceptable by 80% of the people is referred to as the 80% acceptable rate (27.25 °C in Guangzhou). The neutral temperature (24.41 °C in Guangzhou) indicates the minimum temperature necessary for a person to maintain bodily metabolism. In order to quantify thermal comfort among the four tree species, daily PET data in summer are presented in Figure 19. (1) PET in the open area is far greater than the neutral temperature and the 80% acceptable rate. With the exception of a sudden weather change after 14:00 (Figure 19d), almost all PET values were above 30 °C, with large fluctuations. (2) Without considering sudden changes in weather, PET in the shaded area for the four tree species is noticeably lower than that in the open area and is also above the neutral temperature at all times. From 10:00 to 11:00 a.m., however, the PET in the shaded area falls below the 80% acceptable rate, indicating that trees may create a gloomy feeling in the morning when the SR is not too strong. (3) The diurnal variation patterns of PET between trees and under trees are highly consistent. At the same time, when compared to PET under trees, a slightly higher PET with more dramatic fluctuations is found between trees. (4) The inter-tree PETs for *Khaya senegalensis* and *Ficus microcarpa* approach PET at an 80% acceptability rate about 20 min earlier than the under-tree PET and about 1 h earlier than the inter-tree PETs for *Terminalia neotaliala*, *Ficus microcarpa*, and *Mangifera indica*.

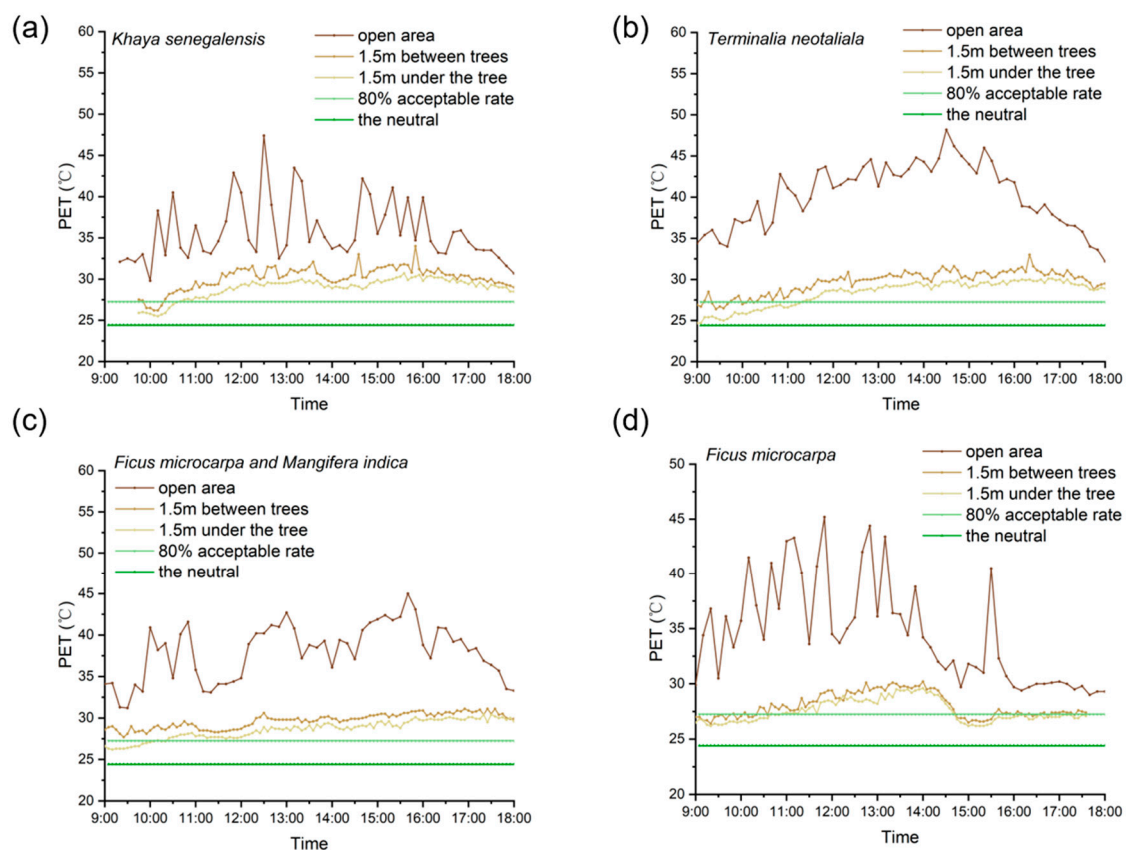


**Figure 19.** Daily variation in PET between trees, under trees, and in the open area at a reference height (1.5 m) for the four tree species. The 80% acceptable rate of PET in Guangzhou is 27.25 °C in summer. The neutral PET in Guangzhou is 24.41 °C in summer. (a) is *Khaya senegalensis*, (b) is *Terminalia neotaliala*, (c) is *Mangifera indica*, and (d) is *Ficus microcarpa*.

Undoubtedly, trees are effective in improving outdoor thermal comfort, and the order of improvement is *Terminalia neotaliala*, *Mangifera indica*, *Ficus microcarpa*, and *Khaya senegalensis* (Figure 20). The greatest improvement benefit is attributed to *Terminalia neotaliala* (12.4 °C, 30.35%), followed by *Ficus microcarpa* and *Mangifera indica* (9.3 °C, 24.16%).

*Ficus microcarpa* (5.95 °C, 17.65%) and *Khaya senegalensis* (5.7 °C, 16.21%) have the least improvement benefit. The difference in  $\Delta$ PET among the various tree species was 0.25 °C.

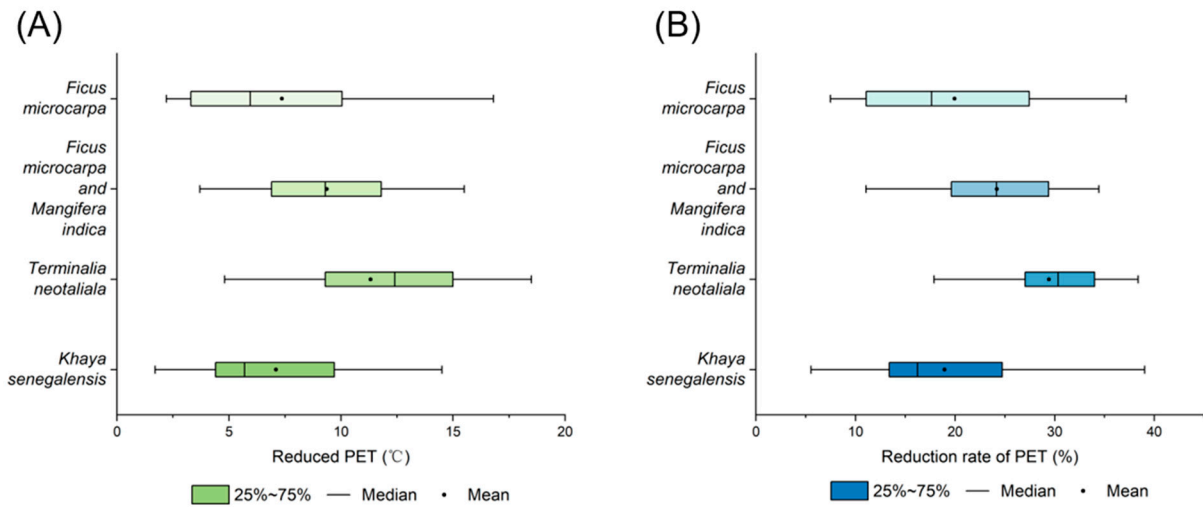


**Figure 20.** Comparison of the PET modification between open and shaded areas among four tree species: (A)  $\Delta$ PET = PET in the open area – PET in the shaded area; (B) reduction rate of PET =  $\Delta$ PET/PET in the open area  $\times$  100%.

The inter-tree and under-tree  $\Delta$ PETs for the four tree species range from 0.5 °C to 1.3 °C (mean 0.98 °C), and the difference rate ranges from 1.83% to 4.47% (mean 3.39%) (Figure 21).

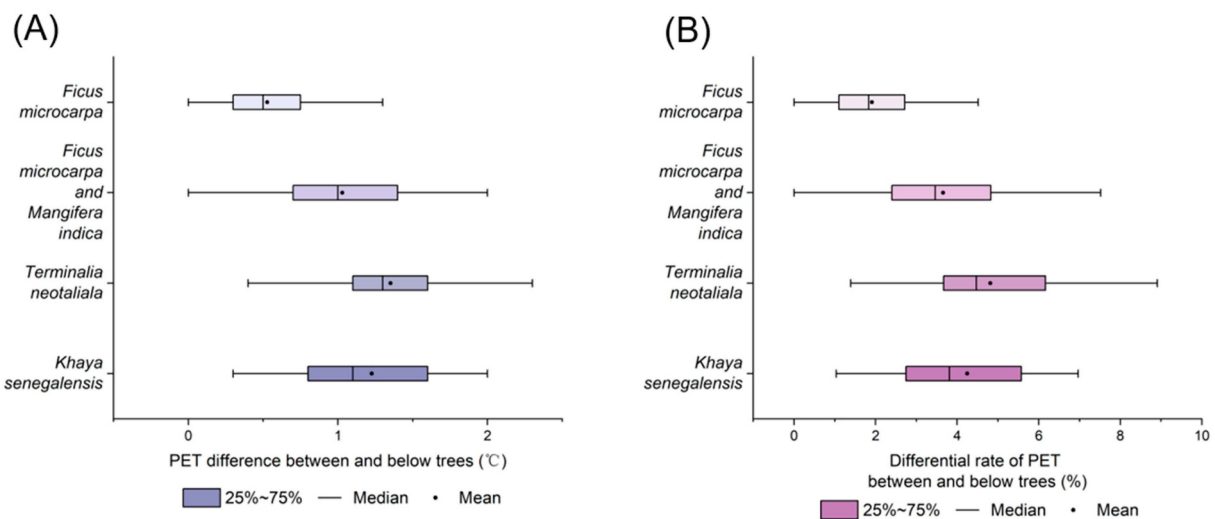


**Figure 21.** Differences between under-tree and inter-tree PET among the four tree species: (A)  $\Delta$ PET = inter-tree PET – under-tree PET; (B) differential rate of PET =  $\Delta$ PET/under-tree PET  $\times$  100%.

### 3.7. Street Orientation

The improvement benefits brought by trees to the outdoor thermal environment with different street orientations are compared and analyzed in terms of the average rates of  $\Delta$ AT,  $\Delta$ ST,  $\Delta$ SR,  $\Delta$ WS, and  $\Delta$ PET (Figure 22). It can be clearly seen that the cooling effect of trees varies by street orientation in the absence of surrounding building shadows. Trees in the NW-SE orientation exhibit the greatest capacity to cool and enhance thermal comfort. The N-S orientation has the next highest cooling performance. The two tree species *Khaya senegalensis* and *Ficus microcarpa* in the NE-SW orientation yield poor cooling benefits. The NW-SE orientation is consistent with the prevailing wind direction in Guangzhou and displays a 16.96% smaller value in  $\Delta$ WS in the shaded area of street trees than in other street



orientations. It is particularly important to improve WS under trees for pedestrian thermal comfort in a high-humidity environment during the transition period. The NW-SE-oriented street trees reduce AT by 3%, ST by 8%, and PET by 14% more than the street trees in the NE-SW orientation. Then, the rate of  $\Delta AT$ ,  $\Delta ST$ , and  $\Delta PET$  values of street trees in the N-S direction are 1.3%, 3%, and 6.5% lower, respectively, than those in the NE-SW orientation.

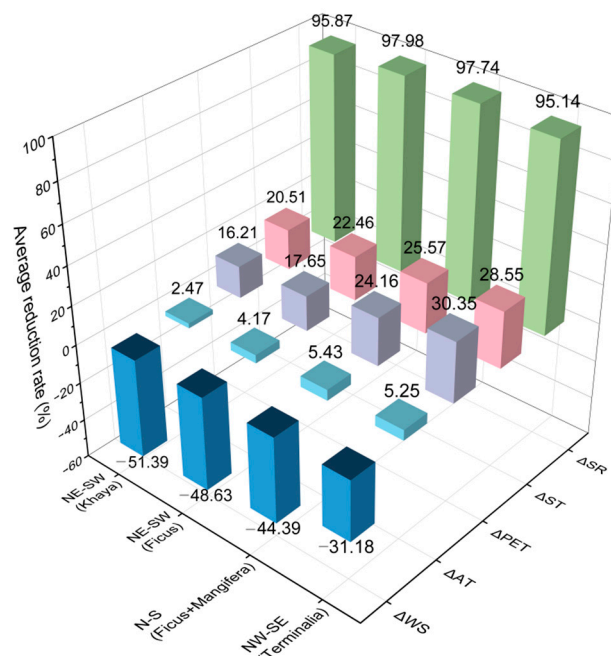


**Figure 22.** Street orientation and the average reduction rates of four parameters:  $\Delta WS$ ,  $\Delta AT$ ,  $\Delta PET$ ,  $\Delta ST$ , and  $\Delta SR$ .

### 3.8. Planting Patterns

As found by others, double-row planting was significantly better than single-row planting. The reduction rate of AT in the NE-SW direction was 1.7 times greater in the double-row *Ficus microcarpa* (4.17%) than in the single-row *Khaya senegalensis* (2.47%). Single-row planting patterns in streets parallel to the prevailing wind direction can also achieve the effect of double-row planting in other orientations. However, the double-row planting pattern in streets (NE-SW) with vertical prevailing winds improves the thermal environment under the canopy even more, increasing the reduction rate of PET by 1.44% compared to single-row planting.

The results also reveal that the planting pattern is the main source of stability in the daily SR variations. The ratio of canopy diameter to plant spacing (D/S) was calculated, and the results are as follows: *Khaya senegalensis* (1.67), *Mangifera indica* (3.10), *Ficus microcarpa* (1.70), and *Terminalia neotaliala* (2.20). Since the D/S ratio of *Khaya senegalensis* is the smallest (1.67), indicating a small canopy diameter and large plant spacing, the SR reduction rate under this tree is unstable. Although the D/S ratio of *Ficus microcarpa* (1.70) is close, the staggered planting pattern of double-row *Ficus microcarpa* makes the shadow distribution between trees uniform and achieves a relatively favorable radiation attenuation effect. Overall, when D/S is greater than 3, the reduction rate of SR under the canopy fluctuates by less than 1%.

## 4. Discussion

### 4.1. Microclimatic Benefits of Street Trees in Transition Seasons

The field measurements and analyses of the microclimatic effects and thermal comfort generated by trees in Guangzhou during the transition season reveal variations among the four tree species in enhancing outdoor microclimates. Regarding air temperature,  $\Delta AT$  for the four tree species ranged from 0.83 °C to 1.82 °C (mean 1.45 °C), and the reduction

rate ranged from 2.47% to 5.43% (mean 4.33%). Numerous studies have explored the cooling benefits of street trees by comparing the air temperature (AT) between shaded and open areas. For example, Lin and Lin determined that in the Cfa climate, air temperatures under the canopy were reduced by 0.64 °C to 2.52 °C during the summer [24]. In Dresden, Germany, trees planted in rows reduced the average air temperatures by 0.77 °C to 2.22 °C during the summer [16]. By comparing the experimentally measured transition season's  $\Delta$ AT with the summer's  $\Delta$ AT reported in the study by Lin and Lin, it is evident that the transition season's  $\Delta$ AT is 0.7 °C lower than that of the summer. The data indicate that street trees provide a significant cooling effect during the transition season. Unlike rows of street trees, the cooling benefit of an individual street tree ranges from 0.85 °C to 1 °C [56].

Humidification by the four tree species varied from 2.41% to 5.26% (average 4.06%). This finding is in agreement with the RH of street trees of 1.11%–6.48% [16]. During the subtropical transition season, RH in the open area generally exceeds 60%. Street trees will raise the RH under the trees due to transpiration, but the increased rate will be limited by the air with high humidity. When the RH in the open area is reduced by 15%, the increased rate of RH in the shaded area rises by around 5%.

$\Delta$ SR for the four tree species varied from 217.67 W/m<sup>2</sup> to 23.75 W/m<sup>2</sup> (average 327.44 W/m<sup>2</sup>), with reduction rates ranging from 95.14% to 97.98% (average 96.68%). As expected, the tree canopy was able to attenuate SR by more than 90% [57], with the LAI as the main factor making a difference among the four tree species [58]. A larger LAI keeps daily SR fluctuation more stable and creates a more uniform shaded area under the canopy.

$\Delta$ ST for the four tree species on the pavement ranged from 8.09 °C to 12.9 °C (mean 10.25 °C), and reduction rates were in the range of 20.51% to 28.55% (mean 24.27%). Previous studies have found that trees may lower soil ST by 3.28 °C to 8.07 °C [24] and asphalt ST by 5.5 °C to 15.2 °C [16]. The reflectivity of various surface materials influences the change in ST, modifying the surface's energy gain [59], which has an impact on the surrounding AT and HTC. Furthermore, with the same street orientation and planting pattern, the  $\Delta$ ST for various species varied around 0.76 °C.

$\Delta$ WS for the four tree species ranged from 0.38 m/s to 0.66 m/s (mean 0.52 m/s), with a reduction rate ranging from 31.18% to 51.39% (mean 43.90%). *Terminalia neotaliala*, being the least obstructive to wind, better meets pedestrian expectations of wind. The WS reduction rates are similar to those found in other studies, which found that cluster-planted trees reduced WS under the trees by 51% to 83% [38], 46% [60], and 54% [61].

$\Delta$ PET for the four tree species varied from 5.7 °C to 12.4 °C (mean 8.34 °C), with reduction rates ranging from 16.21% to 30.35% (mean 22.09%). Maximum improvement benefits were provided by *Terminalia neotaliala*. Street trees have reduced under-tree PET in summer by 4.7 °C to 5.3 °C in Melbourne, Australia [62]; up to 4.6 °C in Freiburg, Germany [63]; 16 °C in Campinas, Brazil [22]; and 16.5 °C in Guangzhou, China [56]. The maximum  $\Delta$ PET among the four tree species in the transition season was approximately 4.1 °C lower than that in the subtropical summer. The minimum  $\Delta$ PET benefit was about 1 °C higher than that in the temperate summer. All four tree species performed well in moderating HTC, but the difference in PET was just 0.25 °C among the four tree species. Consistent with our results, Sanusi concluded that there were no significant differences in PET benefits between tree species [62].

#### 4.2. Under-Tree and Inter-Tree Microclimate Differences

The under-tree and inter-tree microclimate parameters for the four tree species were monitored, and the daily variation curves of AT and RH for each species were found to be close. Their average difference was 0.06 °C for AT and 0.44% for RH. However, the under-tree and inter-tree daily variation curves for SR and ST were more distinct, with differences ranging from 22.01 W/m<sup>2</sup> to 65.37 W/m<sup>2</sup> (mean 48.26 W/m<sup>2</sup>) for SR and 0.1 °C to 1.42 °C (mean 0.91 °C) for ST. Inter-tree and under-tree  $\Delta$ PET among the four tree species ranged from 0.5 °C to 1.3 °C (mean 0.98 °C), with difference rates ranging from 1.83% to 4.47% (mean 3.39%). Inter-tree PET usually reached the 80% acceptable

PET value 20 min to 1 h earlier in the morning, as compared to under-tree PET. The discrepancy in SR and ST between under-tree and inter-tree implies that microclimate parameters are not uniformly distributed under street trees. As a result, while evaluating the overall microclimatic advantages of street trees, the influence of inter-tree variations should be considered.

#### 4.3. Effect of Planting Patterns and Street Orientations on Microclimate Benefits

The double-row planting pattern improves the reduction rate of AT by 1.7 times compared to the single-row planting pattern. The microclimatic benefits of a single-row planting pattern for streets with parallel prevailing winds are comparable to those of street trees planted in a vertical prevailing wind direction. Streets with perpendicular or offset angles to the prevailing wind direction can increase the reduction rate of PET by 1.44% with a double-row planting pattern.

The larger the ratio of canopy diameter to plant spacing ( $D/S$ ), the more consistent the  $\Delta SR$  is under the canopy, indirectly reducing inter-tree and under-tree  $\Delta ST$  differences.  $\Delta SR$  fluctuations under the canopy can be less than 1% at a  $D/S$  ratio of 3 and above. With the same  $D/S$  value, a double-row planting pattern enhanced the stability of the under-tree and inter-tree ST and SR. The reduction rate of SR under the canopy of double-row street trees fluctuated by only 1.3%, which was 1.8 times lower than that in single-row street trees. The difference between under- and inter-tree ST of double-row street trees was roughly 1 °C, while the double-row *Ficus microcarpa* with a staggering planting pattern provided good shade beneath the trees, with a difference of about 0.1 °C.

Trees in the NW-SE orientation were found to have the greatest ability to cool down and improve the microenvironment. Although *Terminalia neotaliala* planted in this orientation did not perform optimally in reducing SR and ST, the NW-SE orientation parallels the prevailing summer wind direction in Guangzhou, thus maintaining a good under-tree microenvironment [64]. The rate of  $\Delta WS$  for *Terminalia neotaliala* in the shaded area was 16.96% lower than that in the other orientations. In hot and humid areas, increasing WS is one of the most effective ways to improve HTC. Street trees planted in the parallel prevailing wind direction (NW-SE) can reduce AT by 5% and PET by 30% on average under the canopy. Conversely, street trees in the NE-SW orientation, perpendicular to the prevailing wind direction, create a poorer thermal environment. Compared to NE-SW, NW-SE has twice the AT reduction rate, while N-S has a 1.3 times more reduction rate than NE-SW. This is in line with Krüger [64], who concluded that trees in S-N-oriented streets can exhibit better cooling potential.

## 5. Limitations

The selected street range was relatively wide, and only a certain area of the street was measured during the experiment. However, since streets change dynamically in real time (e.g., affected by pedestrians, vehicles, etc.), it is recommended that measurement points be arranged in multiple areas of the entire street to obtain more holistic and comprehensive environmental data for the street. Currently, the measured data are applicable to hot and humid areas. In other climatic zones, while the experimental method can be applied, the experimental parameters must be specifically determined according to local conditions, and further relevant studies are required [65–67].

## 6. Conclusions

Based on the physiological parameters of typical tree species in hot and humid areas and their surrounding microclimate data, we have investigated the effects of various tree species, planting patterns, and street orientations on the microclimate under trees, and we have analyzed the changes in the microclimatic parameters of street trees in the transitional season, drawing the following conclusions:

- The four street tree species can significantly improve the thermal environment of street canyons with an average  $\Delta AT$  of 1.45 °C (reduction rate of 4.33%), an average  $\Delta ST$  of 10.25 °C (reduction rate of 24.27%), and an average  $\Delta PET$  of 8.34 °C (reduction rate of 22.09%). In the transition season, the maximum  $\Delta AT$  and  $\Delta PET$  for the four tree species are 1.82 °C and 12.4 °C, respectively, 0.7 °C and 4.1 °C lower than those in the subtropical summer. The minimum  $\Delta PET$  of the four tree species is 5.7 °C, about 1 °C higher than in the temperate summer.
- Based on the potential of the four tree species for improving the outdoor thermal environment, the order of priority is as follows: *Terminalia neotaliala* > *Mangifera indica* > *Ficus microcarpa* > *Khaya senegalensis*. The differences in  $\Delta ST$  and  $\Delta PET$  among the four species were only 0.76 °C and 0.25 °C, respectively.
- Among the four tree species, the inter-tree and under-tree differences averaged 0.06 °C for AT, 0.44% for RH, 0.91 °C for ST and 0.98 °C for PET. Therefore, while evaluating the overall microclimate benefits of street trees, the influence of inter-tree differences should be considered.
- The reduction rate of AT was 1.7 times greater in the double-row planting pattern than in the single-row planting pattern. With the same D/S value, a double-row planting pattern enhanced the stability of the under-tree and inter-tree ST and SR.  $\Delta SR$  fluctuations under the canopy were less than 1% at a D/S ratio of 3 and above.
- In streets parallel to the prevailing summer wind direction (NW-SE) in Guangzhou, street trees in the shaded area yielded a 16.96% reduction in  $\Delta WS$ . Trees in the NE-SW direction had the least ability to improve HTC. Compared to NE-SW, NW-SE had twice the AT reduction rate, while N-S had 1.3 times more reduction rate than NE-SW.
- A single-row planting pattern is recommended for streets with parallel prevailing winds, whereas a double-row planting pattern is better for streets that are perpendicular or at an angle to the prevailing wind direction to improve the HTC.

**Author Contributions:** Conceptualization, S.Z. and X.L.; methodology and formal analysis, S.Z. and X.L.; software, resources, and data curation, S.Z., C.H., and H.X.; validation, S.Z., X.L., C.H., and H.X.; investigation and visualization, S.Z., X.L., C.H., and H.X.; writing—original draft preparation and writing—review and editing, S.Z., X.L., and J.-M.G.; funding acquisition, S.Z. and X.L.; supervision, S.Z., X.L., H.X., and J.-M.G. All authors have read and agreed to the published version of the manuscript.

**Funding:** This research is supported by the National Natural Science Foundation of China (Grant No. 52008115, 51878288 and 52108011); Guangdong Basic and Applied Basic Research Foundation (Grant No. 2023A1515011137 and 2024A1515012129); the 2022 Guangdong Philosophy and Social Science Foundation (Grant No. GD22XGL02); State Key Laboratory of Subtropical Building and Urban Science, South China University of Technology (Grant No. 2024ZB06 and 2021ZB08); Guangzhou Basic and Applied Basic Research Foundation (Grant No. 2024A04J9930); the Department of Housing and Urban–Rural Development of Guangdong Province (Grant No. 2021-K2-305243); and the Department of Education of Guangdong Province (Grant No. 2021KTSCX004).

**Data Availability Statement:** Data will be made available upon request.

**Conflicts of Interest:** The authors declare no conflicts of interest.

## References

1. Halder, B.; Bandyopadhyay, J.; Banik, P. Monitoring the effect of urban development on urban heat island based on remote sensing and geo-spatial approach in Kolkata and adjacent areas, India. *Sustain. Cities Soc.* **2021**, *74*, 103186. [[CrossRef](#)]
2. Yao, L.; Sun, S.; Song, C.; Li, J.; Xu, W.; Xu, Y. Understanding the spatiotemporal pattern of the urban heat island footprint in the context of urbanization, a case study in Beijing, China. *Appl. Geogr.* **2021**, *133*, 102496. [[CrossRef](#)]
3. Liu, H.; Huang, B.; Gao, S.; Wang, J.; Yang, C.; Li, R. Impacts of the evolving urban development on intra-urban surface thermal environment: Evidence from 323 Chinese cities. *Sci. Total Environ.* **2021**, *771*, 144810. [[CrossRef](#)] [[PubMed](#)]
4. Jamei, E.; Rajagopalan, P.; Seyedmahmoudian, M.; Jamei, Y. Review on the impact of urban geometry and pedestrian level greening on outdoor thermal comfort. *Renew. Sustain. Energy Rev.* **2016**, *54*, 1002–1017. [[CrossRef](#)]
5. Mora, C.; Dousset, B.; Caldwell, I.R.; Powell, F.E.; Geronimo, R.C.; Bielecki, C.R.; Counsell, C.W.W.; Dietrich, B.S.; Johnston, E.T.; Louis, L.V.; et al. Global risk of deadly heat. *Nat. Clim. Chang.* **2017**, *7*, 501–506. [[CrossRef](#)]

6. Manoli, G.; Fatichi, S.; Bou-Zeid, E.; Katul, G. Seasonal hysteresis of surface urban heat islands. *Proc. Natl. Acad. Sci. USA* **2020**, *117*, 7082–7089. [[CrossRef](#)] [[PubMed](#)]
7. Liu, X.; Moayed, H.; Ahmadi Dehrashid, A.; Dai, W.; Thi, Q.T. Developments and evolution of housing architecture in the post-Corona era with a health-oriented approach. *Build. Environ.* **2024**, 111936. [[CrossRef](#)]
8. Jamei, Y.; Rajagopalan, P.; Sun, Q. Spatial structure of surface urban heat island and its relationship with vegetation and built-up areas in Melbourne, Australia. *Sci. Total Environ.* **2019**, *659*, 1335–1351. [[CrossRef](#)] [[PubMed](#)]
9. Wang, Z.; Zhao, X.; Yang, J.C.; Song, J.Y. Cooling and energy saving potentials of shade trees and urban lawns in a desert city. *Appl. Energy* **2016**, *161*, 437–444. [[CrossRef](#)]
10. Zhao, Q.; Sailor, D.J.; Wentz, E.A. Impact of tree locations and arrangements on outdoor microclimates and human thermal comfort in an urban residential environment. *Urban For. Urban Green.* **2018**, *32*, 81–91. [[CrossRef](#)]
11. Darvish, A.; Eghbali, G.; Eghbali, S.R. Tree-configuration and species effects on the indoor and outdoor thermal condition and energy performance of courtyard buildings. *Urban Clim.* **2021**, *37*, 100861. [[CrossRef](#)]
12. Manickathan, L.; Defraeye, T.; Allegrini, J.; Derome, D.; Carmeliet, J. Parametric study of the influence of environmental factors and tree properties on the transpirative cooling effect of trees. *Agric. For. Meteorol.* **2018**, *248*, 259–274. [[CrossRef](#)]
13. Meili, N.; Manoli, G.; Burlando, P.; Carmeliet, L.; Chow, W.T.L.; Coutts, A.M.; Roth, M.; Velasco, E.; Vivoni, E.T.; Fatichi, S. Tree effects on urban microclimate: Diurnal, seasonal, and climatic temperature differences explained by separating radiation, evapotranspiration, and roughness effects. *Urban For. Urban Green.* **2021**, *58*, 126970. [[CrossRef](#)]
14. Schlesinger, W.H.; Jasechko, S. Transpiration in the global water cycle. *Agric. For. Meteorol.* **2014**, *189–190*, 115–117. [[CrossRef](#)]
15. Zou, Z.D.; Yang, Y.J.; Qiu, G.Y. Quantifying the Evapotranspiration Rate and Its Cooling Effects of Urban Hedges Based on Three-Temperature Model and Infrared Remote Sensing. *Remote Sens.* **2019**, *11*, 202. [[CrossRef](#)]
16. Gillner, S.; Vogt, J.; Tharang, A.; Dettmann, S.; Roloff, A. Role of street trees in mitigating effects of heat and drought at highly sealed urban sites. *Landsc. Urban Plan.* **2015**, *143*, 33–42. [[CrossRef](#)]
17. Shashua-Bar, L.; Potchter, O.; Bitan, A.; Boltansky, D.; Yaakov, Y. Microclimate modelling of street tree species effects within the varied urban morphology in the Mediterranean city of Tel Aviv, Israel. *Int. J. Climatol.* **2009**, *30*, 44–57. [[CrossRef](#)]
18. Brown, R.D.; Gillespie, T.J. *Microclimate Landscape Design: Creating Thermal Comfort and Energy Efficiency*; John Wiley & Sons: New York, NY, USA, 1995.
19. Deng, J.; Pickles, B.J.; Shao, L. In-situ spectroscopy and shortwave radiometry reveals spatial and temporal variation in the crown-level radiative performance of urban trees. *Remote Sens. Environ.* **2021**, *253*, 112231. [[CrossRef](#)]
20. Coutts, A.M.; White, E.C.; Tapper, N.J.; Beringer, J.; Livesley, S.J. Temperature and human thermal comfort effects of street trees across three contrasting street canyon environments. *Theor. Appl. Climatol.* **2016**, *124*, 55–68. [[CrossRef](#)]
21. Abreu-Harbach, L.V.D.; Labaki, L.C.; Matzarakis, A. Different trees and configuration as microclimate control strategy in Tropics. In Proceedings of the ICUC8—8th International Conference on Urban Climates, Dublin, Ireland, 6–10 August 2012.
22. Abreu-Harbach, L.V.; Labakia, L.C.; Matzarakis, A. Effect of tree planting design and tree species on human thermal comfort in the tropics. *Landsc. Urban Plan.* **2015**, *138*, 99–109. [[CrossRef](#)]
23. Rahman, M.A.; Hartmann, C.; Moser-Reischl, A.; von Strachwitz, M.F.; Paeth, H.; Pretzsch, H.; Pauleit, S.; Rötzer, T. Tree cooling effects and human thermal comfort under contrasting species and sites. *Agric. For. Meteorol.* **2020**, *287*, 107947. [[CrossRef](#)]
24. Lin, B.-S.; Lin, Y.-J. Cooling effect of shade trees with different characteristics in a subtropical urban park. *HortScience* **2010**, *45*, 83–86. [[CrossRef](#)]
25. Morakinyo, T.E.; Kong, L.; Lau, K.K.; Yuan, C.; Ng, E. A study on the impact of shadow-cast and tree species on in-canyon and neighborhood's thermal comfort. *Build. Environ.* **2017**, *115*, 1–17. [[CrossRef](#)]
26. Xiong, Y.; Zhang, J.P.; Xu, X.Y.; Yan, Y.; Sun, S.; Liu, S. Strategies for improving the microclimate and thermal comfort of a classical Chinese garden in the hot-summer and cold-winter zone. *Energy Build.* **2020**, *215*, 109914. [[CrossRef](#)]
27. Leuzingera, S.; Vogt, R.; Körner, C. Tree surface temperature in an urban environment. *Agric. For. Meteorol.* **2010**, *150*, 56–62. [[CrossRef](#)]
28. Yu, Z.W.; Xu, S.B.; Zhang, Y.H.; Jorgensen, G.; Vejre, H. Strong contributions of local background climate to the cooling effect of urban green vegetation. *Sci. Rep.* **2018**, *8*, 6798. [[CrossRef](#)]
29. Hong, B.; Lin, B. Numerical studies of the outdoor wind environment and thermal comfort at pedestrian level in housing blocks with different building layout patterns and trees arrangement. *Renew. Energy* **2015**, *73*, 18–27. [[CrossRef](#)]
30. Hsieh, C.M.; Jan, F.C.; Zhang, L. A simplified assessment of how tree allocation, wind environment, and shading affect human comfort. *Urban For. Urban Green.* **2016**, *18*, 126–137. [[CrossRef](#)]
31. Wu, Z.; Chen, L. Optimizing the spatial arrangement of trees in residential neighborhoods for better cooling effects: Integrating modeling with in-situ measurements. *Landsc. Urban Plan.* **2017**, *167*, 463–472. [[CrossRef](#)]
32. Li, G.; Ren, Z.; Zhan, C. Sky View Factor-based correlation of landscape morphology and the thermal environment of street canyons: A case study of Harbin, China. *Build. Environ.* **2020**, *169*, 106587. [[CrossRef](#)]
33. Krüger, E.; Drach, P.; Emmanuel, R.; Corbella, O. Urban heat island and differences in outdoor comfort levels in Glasgow, UK. *Theor. Appl. Clim.* **2013**, *112*, 127–141. [[CrossRef](#)]
34. Taleghani, M.; Kleerekoper, L.; Tenpierik, M.; van den Dobbelen, A. Outdoor thermal comfort within five different urban forms in the Netherlands. *Build. Environ.* **2014**, *83*, 65–78. [[CrossRef](#)]

35. Fan, C.; Myint, S.W.; Zheng, B. Measuring the spatial arrangement of urban vegetation and its impacts on seasonal surface temperatures. *Prog. Phys. Geogr. Earth Environ.* **2015**, *39*, 199–219. [[CrossRef](#)]
36. Rahman, M.A.; Stratopoulos, L.M.; Moser-Reischl, A.; Zölch, T.; Häberle, K.H.; Rötzer, T.; Pretzsch, H.; Pauleit, S. Traits of trees for cooling urban heat islands: A meta-analysis. *Build. Environ.* **2020**, *170*, 106606. [[CrossRef](#)]
37. Jia, S.; Wang, Y. Effect of heat mitigation strategies on thermal environment, thermal comfort, and walkability: A case study in Hong Kong. *J. Affect. Disord.* **2021**, *201*, 107988. [[CrossRef](#)]
38. Park, M.; Hagishima, A.; Tanimoto, J.; Narita, K.-I. Effect of urban vegetation on outdoor thermal environment: Field measurement at a scale model site. *J. Affect. Disord.* **2012**, *56*, 38–46. [[CrossRef](#)]
39. Zhou, W.; Wang, J.; Cadenasso, M.L. Effects of the spatial configuration of trees on urban heat mitigation: A comparative study. *Remote. Sens. Environ.* **2017**, *195*, 1–12. [[CrossRef](#)]
40. Langenheim, N.; White, M.; Tapper, N.; Livesley, S.J.; Ramirez-Lovering, D. Right tree, right place, right time: A visual-functional design approach to select and place trees for optimal shade benefit to commuting pedestrians. *Sustain. Cities Soc.* **2020**, *52*, 101816. [[CrossRef](#)]
41. Dimoudi, A.; Nikolopoulou, M. Vegetation in the urban environment: Microclimatic analysis and benefits. *Energy Build.* **2003**, *35*, 69–76. [[CrossRef](#)]
42. Lin, T.; Matzarakis, A.; Hwang, R. Shading effect on long-term outdoor thermal comfort. *Build. Environ.* **2010**, *45*, 213–221. [[CrossRef](#)]
43. Cheng, V.; Ng, E.; Chan, C.; Givoni, B. Outdoor thermal comfort study in a sub-tropical climate: A longitudinal study based in Hong Kong. *Int. J. Biometeorol.* **2012**, *56*, 43–56. [[CrossRef](#)]
44. Ng, E.; Cheng, V. Urban human thermal comfort in hot and humid Hong Kong. *Energy Build.* **2012**, *55*, 51–65. [[CrossRef](#)]
45. Mballo, S.; Herpin, S.; Manteau, M.; Demotes-Mainard, S.; Bournet, P. Impact of well-watered trees on the microclimate inside a canyon street scale model in outdoor environment. *Urban Clim.* **2021**, *37*, 100844. [[CrossRef](#)]
46. Liu, Z.; Cheng, W.; Jim, C.; Morakinyo, T.E.; Shi, Y.; Ng, E. Heat mitigation benefits of urban green and blue infrastructures: A systematic review of modeling techniques, validation and scenario simulation in ENVI-met V4. *J. Affect. Disord.* **2021**, *200*, 107939. [[CrossRef](#)]
47. Xiaohan, D.U.; Shi, Y.; Zhang, Y.; Architecture, S.O. Field Study on Thermal Environment of Typical Living Street Canyons in Guangzhou. *Build. Sci.* **2015**, *31*, 8–13. [[CrossRef](#)]
48. Shi, L.; Du, Y.; Zhang, L.; Liu, W. Review of weather and climate characteristics and their impacts in Guangdong Province in May–June 2021. *Guangdong Meteorol.* **2021**, *43*, 2.
49. Li, T. Fairness Evaluation of Urban Forest Based on Ecosystem Services—A Case Study of Guangzhou University City. Master's Thesis, Guangzhou University, Guangzhou, China, 2018.
50. Cai, Y.; Li, C.; Ye, L.; Xiao, L.; Gao, X.; Mo, L.; Du, H.; Zhou, Y.; Zhou, G. Effect of the roadside tree canopy structure and the surrounding on the daytime urban air temperature in summer. *Agric. For. Meteorol.* **2022**, *316*, 108850. [[CrossRef](#)]
51. Huang, F. Influence of Outdoor Thermal Environment Factors on Human Thermal Comfort. Master's Thesis, Central South University, Changsha, China, 2014.
52. Meili, N.; Acero, J.A.; Peleg, N.; Manoli, G.; Burlando, P.; Fatichi, S. Vegetation cover and plant-trait effects on outdoor thermal comfort in a tropical city. *J. Affect. Disord.* **2021**, *195*, 107733. [[CrossRef](#)]
53. Shahidan, M.F.; Shariff, M.K.; Jones, P.; Salleh, E.; Abdullah, A.M. A comparison of *Mesua ferrea* L. and *Hura crepitans* L. for shade creation and radiation modification in improving thermal comfort. *Landsc. Urban Plan.* **2010**, *97*, 168–181. [[CrossRef](#)]
54. Zhang, J.; Gou, Z.; Zhang, F.; Shutter, L. A study of tree crown characteristics and their cooling effects in a subtropical city of Australia. *Ecol. Eng.* **2020**, *158*, 106027. [[CrossRef](#)]
55. Fahmy, M.; Sharples, S.; Yahiya, M. LAI based trees selection for mid latitude urban developments: A microclimatic study in Cairo, Egypt. *J. Affect. Disord.* **2010**, *45*, 345–357. [[CrossRef](#)]
56. Zheng, S.; Guldmann, J.-M.; Liu, Z.; Zhao, L. Influence of trees on the outdoor thermal environment in subtropical areas: An experimental study in Guangzhou, China. *Sustain. Cities Soc.* **2018**, *42*, 482–497. [[CrossRef](#)]
57. Zhao, X.; Li, G.; Gao, T. Thermal Comfort Effects and Morphological Characteristics of Typical Street Trees in Summer in Harbin. *Landsc. Archit.* **2016**, *12*, 74–80. [[CrossRef](#)]
58. Gebert, L.; Coutts, A.; Tapper, N. The influence of urban canyon microclimate and contrasting photoperiod on the physiological response of street trees and the potential benefits of water sensitive urban design. *Urban For. Urban Green.* **2019**, *40*, 152–164. [[CrossRef](#)]
59. Lee, H.; Holst, J.; Mayer, H. Modification of Human-Biometeorologically Significant Radiant Flux Densities by Shading as Local Method to Mitigate Heat Stress in Summer within Urban Street Canyons. *Adv. Meteorol.* **2013**, *2013*, 1–13. [[CrossRef](#)]
60. Heisler, G.M. Mean wind speed below building height in residential neighborhoods with different tree densities. *ASHRAE Trans.* **1990**, *96*, 1389–1396.
61. DeWalle, D.R.; Heisler, G.M. Windbreak effects on air infiltration and space heating in a mobile home. *Energy Build.* **1983**, *5*, 279–288. [[CrossRef](#)]
62. Sanusi, R.; Johnstone, D.; May, P.; Livesley, S.J. Microclimate benefits that different street tree species provide to sidewalk pedestrians relate to differences in Plant Area Index. *Landsc. Urban Plan.* **2017**, *157*, 502–511. [[CrossRef](#)]

63. Mayer, H.; Kuppe, S.; Holst, J.; Imbery, F.; Matzarakis, A. *Human Thermal Comfort Below the Canopy of Street Trees on a Typical Central European Summer Day*; Reports of the Meteorological Institute; Albert-Ludwigs-University: Freiburg, Germany, 2009; Volume 18, pp. 211–219.
64. Krüger, E.; Pearlmutter, D.; Rasia, F. Evaluating the impact of canyon geometry and orientation on cooling loads in a high-mass building in a hot dry environment. *Appl. Energy* **2010**, *87*, 2068–2078. [[CrossRef](#)]
65. Liu, X.; He, J.; Xiong, K.; Liu, S.; He, B.-J. Identification of factors affecting public willingness to pay for heat mitigation and adaptation: Evidence from Guangzhou, China. *Urban Clim.* **2023**, *48*, 101405. [[CrossRef](#)]
66. Liu, S.; Wang, Y.; Liu, X.; Yang, L.; Zhang, Y.; He, J. How does future climatic uncertainty affect multi-objective building energy retrofit decisions? Evidence from residential buildings in subtropical Hong Kong. *Sustain. Cities Soc.* **2023**, *92*, 104482. [[CrossRef](#)]
67. Li, K.; Liu, X.; Zhang, H.; Ma, J.; He, B.-J. Evaluating and improving the adaptability of commonly used indices for predicting outdoor thermal sensation in hot and humid residential areas of China. *Dev. Built Environ.* **2023**, *16*, 100278. [[CrossRef](#)]

**Disclaimer/Publisher’s Note:** The statements, opinions and data contained in all publications are solely those of the individual author(s) and contributor(s) and not of MDPI and/or the editor(s). MDPI and/or the editor(s) disclaim responsibility for any injury to people or property resulting from any ideas, methods, instructions or products referred to in the content.